Microlocal Properties of Dynamic Fourier Integral Operators

Bernadette N. Hahn, Melina-L. Kienle Garrido, and Eric Todd Quinto

Abstract Following from the previous chapter *Motion compensation strategies in tomography*, this article provides a complementary study on the overall information content in dynamic tomographic data using the framework of microlocal analysis and Fourier integral operators. Based on this study, we further analyze which characteristic features of the studied specimen can be reliably reconstructed from dynamic tomographic data and which additional artifacts have to be expected in a dynamic image reconstruction. Our theoretical results, in particular the affect of the dynamic behavior on the measured data and the reconstruction result, is then illustrated in detail at various numerical examples from dynamic photoacoustic tomography.

1 On Singularities and Artifacts

In the previous chapter *Motion compensation strategies in tomography* [16], we studied regularization strategies for solving time-dependent inverse problems in tomography, which arise when the investigated specimen changes during the data acquisition process. In this article, we now provide a complementary study on the overall information content of such dynamic tomography data. In particular, we show how the respective information content affects the reconstruction quality.

Typically, the searched-for quantity f in tomographic applications can be considered as a piecewise constant function, where each value represents a specific material (e.g. bone, brain, air, etc.). In this case, the gradient ∇f–or more precisely the *singularities* of f–contain much of the information about f. A rigorous

B. N. Hahn (✉) · M.-L. Kienle Garrido
Department of Mathematics, University of Stuttgart, Stuttgart, Germany
e-mail: bernadette.hahn@imng.uni-stuttgart.de;
Melina-Loren.Kienle-Garrido@imng.uni-stuttgart.de

E. T. Quinto
Department of Mathematics, Tufts University, Medford, MA, USA
e-mail: todd.quinto@tufts.edu

B. Kaltenbacher et al. (eds.), *Time-dependent Problems in Imaging and Parameter Identification*, https://doi.org/10.1007/978-3-030-57784-1_4

mathematical definition of singularity is given in Sect. 2 along with an intuitive example.

The task "finding f from measured data $g = \mathcal{A}f$" then corresponds to "extracting the singular features of f from g". Thus, a thorough analysis on how an operator $\mathcal{A}$ encodes singular features has to be developed in order to fully understand the reconstruction process. This in turn can provide important insights regarding the design of reconstruction operators in order to avoid the formation of unwanted artifacts in the resulting reconstruction.

The most prominent example is limited-angle computerized tomography. In various applications, the radiation source cannot perform a complete 180- or 360° rotation around the specimen, such as for instance in dental diagnostics. If data are only measured for a subinterval of this angular range, the standard CT-reconstruction algorithm causes additional features, namely streak artifacts, to appear in the reconstruction results, see Figs. 2 and 3. Furthermore, certain singular features are missing in the reconstructed image.

An analysis of singularities and artifacts requires deep mathematics, namely the theory of *microlocal analysis* which goes back to techniques developed by Hörmander and others based on Fourier transforms. Over the last decades, microlocal analysis has been employed to understand image formation in static tomographic problems such as classical X-ray CT [9, 27, 31], seismics [5, 11, 29], sonar [10, 25], radar [1, 6, 28, 36], electron microscope tomography [32], Compton CT [34, 39], and geodesic transforms [8, 19].

In this article, we extend these classic results to dynamic tomography problems. In particular, we tackle the following questions:

- How does the dynamic behavior of the object affect the information content of the data g?
- Which singular features can be reliably reconstructed from dynamic tomography data?
- Which additional artifacts have to be expected in a dynamic image reconstruction?

Such a rigorous mathematical characterization can have great benefits in applications. For instance, it allows radiologists to determine whether a singularity in the reconstructed image belongs to the object or represents an artifacts, thereby making more reliable medical diagnoses. It could further serve as a basis for developing an adaptive data sampling protocol depending on the motion of the patient so that the measurements encode all relevant information. The analysis based on the model operator $\mathcal{A}$ could also be combined with data driven methods for image reconstruction or image post-processing in order to guarantee reliable results.

Microlocal analysis has begun to be used in motion-compensated CT [18, 22, 23] with extensions to generalized dynamic Radon transforms [17, 33]. The aim of this article is to provide a general framework for dynamic Fourier integral operators along with a characterization of visible singularities and added artifacts.

With this aim in mind, the article is organized as follows. In Sect. 2, we provide the basic concepts from microlocal analysis, including the concepts of singularities,

Fourier integral operators and artifacts. Next, in Sect. 3, we derive the concept of dynamic Fourier integral operators based on an underlying motion model, and we study how these operators encode the singularities of the searched-for quantity in the measured data. Due to their practical relevance in tomography, we provide, in particular, a detailed analysis for the special case of generalized dynamic Radon transforms. Section 4 addresses the reconstruction problem assuming the motion is known exactly. In particular, we characterize visible and added singularities in dynamic reconstructions using methods of filtered backprojection type. Our theoretical results are then illustrated in Sect. 5 for various numerical examples from dynamic photoacoustic tomography (PAT).

2 Basic Concepts of Microlocal Analysis

In this section we will outline the basic microlocal principles used in the article. We refer to [20, 21, 24, 37, 38] for more details.

First, we introduce some basic notation. Let $x = (x_1, x_2)$ be in $\mathbb{R}^2$ and let h be a real-valued function of variables including x. Let $G = (g_1, g_2)^T$ be an $\mathbb{R}^2$-valued function of variables including x. Then we define

$$D_x h = \left(\frac{\partial h}{\partial x_1}, \frac{\partial h}{\partial x_2} \right), \qquad D_x G = \begin{pmatrix} \frac{\partial g_1}{\partial x_1} & \frac{\partial g_1}{\partial x_2} \\ \frac{\partial g_2}{\partial x_1} & \frac{\partial g_2}{\partial x_2} \end{pmatrix} = \begin{pmatrix} D_x g_1 \\ D_x g_2 \end{pmatrix}$$

and other derivatives are defined in a similar way; for example, if h depends on t, then we define $D_t h = \frac{\partial h}{\partial t}$.

We now introduce notation for higher derivatives. Let $n \in \mathbb{N}$, then the point $\overline{\boldsymbol{\alpha}} = (\alpha_1, \alpha_2, \ldots, \alpha_n) \in \{0, 1, 2, \ldots\}^n$ is called a *multi-index*. Let Ω be an open subset of $\mathbb{R}^n$ and let $h : \Omega \to \mathbb{R}$ be smooth. Then we define

$$\begin{aligned} D^{\overline{\boldsymbol{\alpha}}} h &= \frac{\partial^{\alpha_1}}{\partial x_1^{\alpha_1}} \frac{\partial^{\alpha_2}}{\partial x_2^{\alpha_2}} \cdots \frac{\partial^{\alpha_n}}{\partial x_n^{\alpha_n}} h \quad \text{and} \\ |\overline{\boldsymbol{\alpha}}| &= \alpha_1 + \alpha_2 + \cdots \alpha_n. \end{aligned} \tag{1}$$

Now, we introduce some basic function classes. The set $\mathcal{D}(\mathbb{R}^n)$ consists of all C^∞ smooth functions of compact support in $\mathbb{R}^n$ and $f_k \to f$ in $\mathcal{D}(\mathbb{R}^n)$ if for some fixed compact set K, all f_k are supported in K and $f_k \to f$ uniformly along with all derivatives. The set $\mathcal{E}(\mathbb{R}^n)$ is the set of all C^∞ smooth functions on $\mathbb{R}^n$ with convergence in $\mathcal{E}$ being uniform convergence on compact sets along with all derivatives.

The dual space to $\mathcal{D}(\mathbb{R}^n)$ is denoted $\mathcal{D}'(\mathbb{R}^n)$ and called the space of distributions. Its topology is defined by weak convergence (i.e., $u_k \to u$ in $\mathcal{D}'(\mathbb{R}^n)$ if for every $f \in \mathcal{D}(\mathbb{R}^n)$, $u_k(f) \to u(f)$). The dual space to $\mathcal{E}(\mathbb{R}^n)$ is the set $\mathcal{E}'(\mathbb{R}^n)$ of all distributions of compact support with the topology defined by weak convergence on functions in $\mathcal{E}(\mathbb{R}^n)$. More details on these function spaces can be found, e.g., in [35].

2.1 A Rigorous Theory of Singularities

Wavefront sets are a precise classification of singularities of functions and the key to understanding them is the relation between smoothness of f and rapid decay at infinity of its Fourier transform, $\mathcal{F}f(y) = \frac{1}{2\pi}\int_{x\in\mathbb{R}^2} e^{-iy\cdot x} f(x)\mathrm{d}x$.

Smoothness and Rapid Decay
A distribution $f \in \mathcal{E}'(\mathbb{R}^n)$ is smooth if and only if $\mathcal{F}f$ is rapidly decaying at infinity (i.e., $\mathcal{F}f(\xi)$ decays at infinity faster than any power of $1/\|\xi\|$).

The proof of this statement uses the Fourier inversion formula [35], boundedness of $\mathcal{F}\colon L^1(\mathbb{R}^n) \to L^\infty(\mathbb{R}^n)$, and that, under the Fourier transform, a derivative of f becomes the product of a polynomial with $\mathcal{F}f$.

Definition 1 Let $u \in \mathcal{D}'(\mathbb{R}^n)$ and let $(x_0, \xi_0) \in \mathbb{R}^n \times (\mathbb{R}^n \setminus \{\mathbf{0}\})$. Then u is smooth at x_0 in direction ξ_0 if there is a smooth cutoff function at x_0, $\psi \in \mathcal{D}(\mathbb{R}^n)$ (i.e., $\psi(x_0) \neq 0$) and an open cone V containing ξ_0 such that $\mathcal{F}(\psi u)(\xi)$ is rapidly decaying at infinity for all $\xi \in V$.

On the other hand, if u is not smooth at x_0 in direction ξ_0, then $(x_0, \xi_0) \in \mathrm{WF}(u)$, the C^∞ wavefront set of u.

This definition generalizes the relation between rapid decay of $\mathcal{F}f$ and smoothness of f by considering decay near individual directions rather than in all directions. Generally, the wavefront set is defined as a subset of a cotangent bundle, but we will not use that abstraction since there is a natural identification of $\mathbb{R}^n \times (\mathbb{R}^n \setminus \{\mathbf{0}\})$ with $T^*(\mathbb{R}^n) \setminus \{\mathbf{0}\}$.

In particular, according to its definition, the vectors $(x_0, \xi_0) \in \mathrm{WF}(u)$ characterize simultaneously the location, $x_0 \in \mathbb{R}^n$, and the direction, $\xi_0 \in \mathbb{R}^n \setminus \{\mathbf{0}\}$ of singularities of f.

Example
The wavefront sets of characteristic functions can be understood intuitively.

First, let D be the unit disk in $\mathbb{R}^2$ and let χ_D, be its characteristic function. Note that χ_D is smooth (either identically zero or identically one) away from the boundary of D, namely the unit sphere S^1. Therefore, the wavefront set $\mathrm{WF}(\chi_D)$ should involve only points x in this boundary. In fact, $\mathrm{WF}(\chi_D)$ is the set of normals to the boundary of the disk,

$$\left\{(x, tx) \,\middle|\, x \in S^1, t \neq 0\right\}$$

(continued)

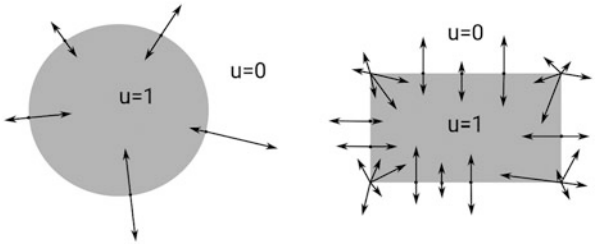

Fig. 1 An illustration of WF(u) when $u = \chi_D$ is the characteristic function of the unit disk D (left) and when $u = \chi_R$ is the characteristic function of a rectangle R (right)

as illustrated in Fig. 1 (left). Intuitively, these normal vectors point in the direction of greatest "non-smoothness."

If S is an arbitrary set with smooth boundary, then the wavefront set of χ_S consists of all normals to the boundary of S.

If the set S has a corner, then the wavefront set of χ_S will include all vectors at the corner. For example, the wavefront set of the characteristic function χ_R of a rectangle R will include all normal vectors along the edges of the rectangle and all vectors at the vertices of the rectangle, see Fig. 1 (right).

In general, if u is not smooth at a point x, then u has wavefront set above x; that is, for some $\xi \in \mathbb{R}^2 \setminus \{\mathbf{0}\}$, $(x, \xi) \in \mathrm{WF}(u)$.

The following theorem will be important to analyze added artifacts.

Theorem 1 ([21, Theorem 8.2.10]) *Let Ω_1 be an open set in $\mathbb{R}^n$ and let $u \in \mathcal{E}'(\Omega_1)$. If the following* non-cancellation condition *holds*

$$\forall (z, \xi) \in \mathrm{WF}(u) : \quad (z, -\xi) \notin \mathrm{WF}(\chi_B), \tag{2}$$

then the product $\chi_B u$ can be defined as a distribution. In this case,

$$\mathrm{WF}(\chi_B u) \subset Q(B, \mathrm{WF}(u)),$$

where for $W \subset \Omega_1 \times \mathbb{R}^n \setminus \{\mathbf{0}\}$

$$Q(B, W) := \{(z, \xi + \eta) \,\big|\, z \in B, [(z, \xi) \in W \vee \xi = 0] \wedge [(z, \eta) \in \mathrm{WF}(\chi_B) \vee \eta = 0]\}.$$

2.2 Fourier Integral Operators

In this section, we define the fundamental classes of operators on which our analysis is based. Note that we do not give the general definitions but ones that are sufficient for our purposes. In particular, we consider two-dimensional imaging problems in this article, i.e. we set the dimension to $n = 2$ in the following. For other applications, one would use the definition for general spaces in [38, Chapter VI.2] or [20]. These operators are defined in terms of amplitudes and we start with this definition.

Definition 2 (Amplitude of Order k) Let Ω_1 and Ω_2 be open sets in $\mathbb{R}^2$ and let $m \in \{1, 2\}$. Now let $a(z, x, \tau)$ be a smooth function on $\Omega_1 \times \Omega_2 \times \mathbb{R}^m$. Then a is an *amplitude of order k* if it satisfies the following condition. For each compact subset K in $\Omega_1 \times \Omega_2$ and each $M \in \mathbb{N}$, there exists a positive constant $C_{K,M}$ such that

$$\left| D_z^{\overline{\boldsymbol{\alpha}}} D_x^{\overline{\boldsymbol{\beta}}} D_\tau^{\overline{\boldsymbol{\gamma}}} a(z, x, \tau) \right| \leq C_{K,M} (1 + \|\tau\|)^{k - |\overline{\boldsymbol{\gamma}}|} \tag{3}$$

for all $(z, x, \tau) \in K \times \mathbb{R}^m$ whenever $|\overline{\boldsymbol{\alpha}}| + \left|\overline{\boldsymbol{\beta}}\right| + |\overline{\boldsymbol{\gamma}}| \leq M$.

We now define the general class of operators we consider in this article.

Definition 3 (Fourier Integral Operator (FIO)) Let $m \in \{1, 2\}$ and let Ω_1 and Ω_2 be open subsets of $\mathbb{R}^2$. The real-valued function $\Phi = \Phi(z, x, \tau) \in C^\infty(\Omega_1 \times \Omega_2 \times (\mathbb{R}^m \setminus \{\mathbf{0}\}))$ is called a *phase function* if Φ is positive homogeneous of degree 1 in the phase variable τ. We define

$$\Sigma_\Phi = \left\{ (z, x, \tau) \in \Omega_1 \times \Omega_2 \times \mathbb{R}^m \setminus \{\mathbf{0}\} \;\middle|\; D_\tau \Phi = 0 \right\} \tag{4}$$

and we call the phase function Φ *non-degenerate* if

$$D_z \Phi \text{ and } D_x \Phi \text{ are both nonzero for all } (z, x, \tau) \in \Sigma_\Phi. \tag{5}$$

Now let $a(z, x, \tau)$ be an amplitude (see Definition 2) of order k and let Φ be a non-degenerate phase function.

The operator $\mathcal{T}$ defined for $u \in \mathcal{E}'(\Omega_2)$ by

$$\mathcal{T}u(z) = \int e^{i\Phi(z,x,\tau)} a(z, x, \tau) u(x) \mathrm{d}x \, \mathrm{d}\tau \tag{6}$$

is a *Fourier Integral Operator (FIO)* of order $k + (m - 2)/2$.

The *canonical relation* for $\mathcal{T}$ is

$$C := \left\{ (z, D_z \Phi(z, x, \tau); x, -D_x \Phi(z, x, \tau)) \;\middle|\; (z, x, \tau) \in \Sigma_\Phi \right\}. \tag{7}$$

Since the phase function Φ satisfies (5), the sets Σ_Φ and C are smooth manifolds.

Example (Radon Transform)
The mathematical model of computerized tomography is given by the classical *Radon transform*

$$\mathcal{R}u(\varphi, s) = \int u(x)\delta(s - x^T\theta(\varphi))\,\mathrm{d}x,$$

which integrates u along the straight lines

$$\left\{x \in \mathbb{R}^2 \,\middle|\, x^T\theta(\varphi) = s\right\}$$

with $\theta(\varphi) = (\cos\varphi, \sin\varphi)^T$ and δ the delta-distribution. Note that $\Omega_1 = [0, 2\pi] \times \mathbb{R}$ with 0 and 2π identified in this case; therefore the data variable $z \in \Omega_1$ has been replaced by $(\varphi, s) \in [0, 2\pi] \times \mathbb{R}$. This operator is an FIO of order $-1/2$ with phase variable $\tau \in \mathbb{R} \setminus \{\mathbf{0}\}$ and representation

$$\mathcal{R}u(\varphi, s) = \int e^{i\tau(s - x^T\theta(\varphi))} \frac{1}{2\pi} u(x)\,\mathrm{d}x\,\mathrm{d}\tau,$$

where the phase function is $\Phi(\varphi, s, x, \tau) = \tau(s - x^T\theta(\varphi))$ and the amplitude is $a(\varphi, s, x, \tau) = \frac{1}{2\pi}$, which is a symbol of order zero. Note that this Fourier representation of $\mathcal{R}$ is valid by the Fourier Slice Theorem (e.g., [26, Theorem 1.1]).

Example (Pseudodifferential Operators (PSIDOs))
We now define a special type of FIO. In this case, $m = 2$ and the phase variable will be denoted $\xi \in \mathbb{R}^2$. Let Ω be an open subset of $\mathbb{R}^2$.

Let the function $a(z, x, \xi)$ for $(z, x, \xi) \in \Omega \times \Omega \times \mathbb{R}^2$ be an amplitude satisfying Definition 2. Define

$$\Phi(z, x, \xi) = \xi \cdot (z - x),$$

then Φ is a phase function satisfying the non-degeneracy condition (5).

Under these conditions the *pseudodifferential operator (PSIDO)*

$$\mathcal{P}u(z) = \int e^{i\Phi(z,x,\xi)} a(z, x, \xi)u(x)\,\mathrm{d}x\,\mathrm{d}\xi$$

is an FIO satisfying Definition 3.

(continued)

Note that, if the amplitude a has order k, then $\mathcal{P}$ is an FIO of order k associated to the canonical relation

$$\Delta = \left\{(x, \xi, x, \xi) \,\middle|\, (x, \xi) \in \Omega \times \left(\mathbb{R}^2 \setminus \{\mathbf{0}\}\right).\right\}$$

Every smooth differential operator is a PSIDO, and its order as a PSIDO is the same as its order as a differential operator.

2.3 FIO and Wavefront Sets

To state the theorems that describe how operators change wavefront sets, we need the following definitions. Let X and Y be sets and let $B \subset X \times Y$, $C \subset Y \times X$, and $D \subset X$. Then, we define

$$\begin{aligned} C^t &:= \left\{(x, y) \,\middle|\, (y, x) \in C\right\} \\ C \circ D &:= \left\{y \in Y \,\middle|\, \exists x \in D, (y, x) \in C\right\} \\ B \circ C &:= \left\{(x', x) \in X \times X \,\middle|\, \exists y \in Y, (x', y) \in B,\ (y, x) \in C\right\}, \end{aligned} \tag{8}$$

and

$$\begin{aligned} \Pi_L &: C \to Y, \quad \Pi_L(y, x) = y \\ \Pi_R &: C \to X, \quad \Pi_R(y, x) = x \end{aligned}$$

are the natural projections from C.

Next, we note that the formal dual of an FIO is an FIO.

Theorem 2 ([20, Theorem 4.2.1]) *Let $\mathcal{T}$ be an FIO of order k with canonical relation C. Then the formal dual operator, $\mathcal{T}^*$ to $\mathcal{T}$ is an FIO of order k with canonical relation C^t.*

The next definition is helpful to determine which singularities are visible, as we will discuss in the next section.

Definition 4 Let $\mathcal{T}$ be an FIO given by (6) with amplitude a of order k. Then $\mathcal{T}$ is *elliptic* if its amplitude a satisfies the following condition. For each compact set $K \subset \Omega_1 \times \Omega_2$ there are constants $C_K > 0$ and $S_K > 0$ such that for all $(z, x) \in K$ and for all $\tau \in \mathbb{R}^m$ such that $\|\tau\| > S_K$,

$$|a(z, x, \tau)| \geq C_K (1 + \|\tau\|)^k.$$

Our next definition is fundamental for our results.

Definition 5 Let $\mathcal{T}$ be an FIO with canonical relation C. Then, $\mathcal{T}$ satisfies the *semi-global Bolker Assumption* if the natural projection $\Pi_L : C \to \Omega_1 \times \mathbb{R}^2 \setminus \{\mathbf{0}\}$ is an embedding–a smooth injective map with injective derivative.

Victor Guillemin [12, 14] called Definition 5 plus additional geometric conditions (including that $\mathcal{T}$ is a Radon transform defined by a double fibration for which the projection to X is proper, and Π_R is surjective) the Bolker Assumption. His extra conditions assure that one can compose $\mathcal{T}^*$ and $\mathcal{T}$ and that the composition is an elliptic pseudodifferential operator. This is not true in general without extra assumptions.

A straightforward calculation shows that PSIDOs satisfy the semi-global Bolker Assumption.

FIOs transform wavefront sets in precise ways, and our next theorem, a special case of the Hörmander-Sato Lemma, is a key to our analysis.

Theorem 3 ([20, Theorems 2.5.7 and 2.5.14], [38, Section 6.3, (6.22)]) *Let $\mathcal{T}$ be an FIO (Definition 3) with canonical relation C. Let $f \in \mathcal{E}'(\Omega_2)$. Then*

$$\mathrm{WF}(\mathcal{T}f) \subset C \circ \mathrm{WF}(f). \tag{9}$$

If $\mathcal{T}$ is elliptic and satisfies the semi-global Bolker Assumption, then equality holds in (9).

For PSIDOs, this theorem implies that $\mathrm{WF}(\mathcal{P}(f)) \subset \mathrm{WF}(f)$ and equality holds if $\mathcal{P}$ is elliptic since the canonical relation of PSIDOs is Δ.

We will need several continuity results for FIOs.

Theorem 4 ([21, Theorem 8.2.13]) *Let $\mathcal{T}$ be an FIO satisfying Definition 3. Then $\mathcal{T} : \mathcal{E}'(\Omega_2) \to \mathcal{D}'(\Omega_1)$ is weakly continuous.*

Therefore, if $\mathcal{P}$ is a PSIDO satisfying the conditions in the Example on Pseudodifferential Operators , then $\mathcal{P} : \mathcal{E}'(\Omega) \to \mathcal{D}'(\Omega)$ is weakly continuous.

Theorem 4 is valid because we assume (5) in the definition of FIO, and this condition holds for the phase function for PSIDO. In general, FIOs are continuous in Sobolev scale. Before stating our theorem, we provide some definitions.

Definition 6 Let Ω be an open subset of $\mathbb{R}^2$. The set $H_c^s(\Omega)$ is the set of all distributions u with compact support in Ω such that the Sobolev norm

$$\|u\|_s = \sqrt{\int_{\xi \in \mathbb{R}^2} \mathcal{F}u(\xi) \left(1 + \|\xi\|^2\right)^s \, \mathrm{d}\xi}$$

is finite.

The set $H^s_{\mathrm{loc}}(\Omega)$ is the set of all distributions u supported in Ω such that for all cutoff functions $\varphi \in \mathcal{D}(\Omega)$, $\varphi u \in H_c^s(\Omega)$.

We say a linear operator $A : H_c^s(\Omega_2) \to H_{\text{loc}}^{s-k}(\Omega_1)$ is continuous if for each fixed compact set $K \subset \Omega_2$ and each $\varphi \in \mathcal{D}(\Omega_1)$, there is a constant $C_{K,\varphi} > 0$ such that for all $u \in \mathcal{E}'(\Omega_2)$ supported in K,

$$\|\varphi A u\|_{s-k} \leq C_{K,\varphi} \|u\|_s .$$

Theorem 5 ([20, Theorem 4.3.1]) *Let $\mathcal{T}$ be an FIO of order $k \in \mathbb{R}$ and assume the projection $\Pi_L : C \to \Omega_1 \times \mathbb{R}^2$ is an immersion (i.e. the derivative of Π_L is injective). Then*

$$\mathcal{T} : H_c^s(\Omega_2) \to H_{loc}^{s-k}(\Omega_1)$$

is continuous.

Therefore, if $\mathcal{A}$ is a PSIDO of order k then $\mathcal{A} : H_c^s(\Omega) \to H_{\text{loc}}^{s-k}(\Omega)$ is continuous.

Note that the condition in this theorem about Π_L will be true whenever $\mathcal{T}$ satisfies the semi-global Bolker Assumption.

2.4 Visible Singularities and Artifacts

In the rest of the article, the reconstruction operators we consider will be either regular PSIDOs or PSIDO-like operators that have discontinuous symbols, and we will use the theory of singularities and FIOs developed in this section to describe what these operators can do to singularities of the object in the reconstruction step. We now provide the basic terminology to describe this.

Definition 7 Let $\mathcal{L}$ be a reconstruction operator, $f \in \mathcal{E}'(\mathbb{R}^2)$, and $(x, \xi) \in \text{WF}(f)$.

Then, (x, ξ) will be a singularity of f that is visible in the reconstruction or *visible singularity* if $(x, \xi) \in \text{WF}(\mathcal{L}f)$.

On the other hand, (x, ξ) will be an *invisible singularity* of f if $(x, \xi) \notin \text{WF}(\mathcal{L}f)$.

Any singularity $(y, \eta) \in \text{WF}(\mathcal{L}f)$ that is not in $\text{WF}(f)$ will be called an *artefact*.

This terminology is illustrated using two examples from static 2D-CT. According to the inversion formula of the Radon transform, all singularities of f can be recovered via a filtered backprojection algorithm, if data are collected for $\varphi \in [0, \pi]$, [26]. However, if a only a smaller angular range can be covered, certain singularities will be invisible in the reconstruction and streak artifacts arise instead [31]. This is illustrated in Fig. 2 for the Shepp-Logan phantom with $\varphi \in [0, \frac{3}{4}\pi]$ and in Fig. 3 for a circular phantom with $\varphi \in [0, \frac{\pi}{2}]$ (left). For this circular phantom, the visible/invisible singularities and the added artifacts are highlighted in Fig. 3 (right).

A detailed analysis of visible and invisible singularities as well as added artifacts in dynamic image reconstruction is provided in Sect. 4.

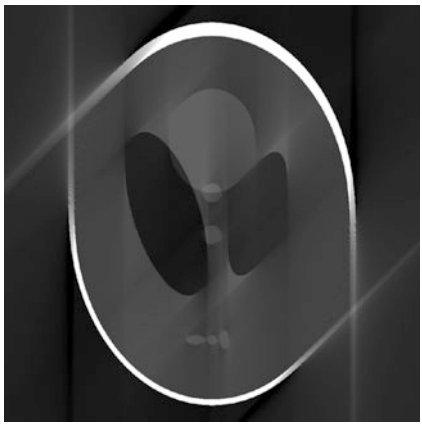

Fig. 2 Shepp-Logan Phantom reconstructed from 2D CT-data with limited angular range $[0, \frac{3}{4}\pi]$

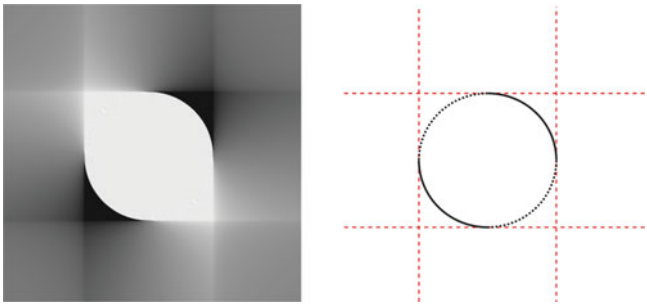

Fig. 3 Left: Circular phantom reconstructed from "D-CT data with limited angular range $[0, \frac{\pi}{2}]$. Right: Visible singularities (solid line), invisible singularities (dotted line) and added artifacts (dashed line) for a circular phantom

3 Encoding Object Singularities in Dynamic Imaging Data

In this section, we analyze how singularities of a moving object get encoded in dynamic imaging data. Therefore, we first recall the motion model developed in the chapter *Motion compensation strategies in tomography* [16] and the mathematical characterization for our moving object.

Let $[0, T]$, $T \in \mathbb{R}_{>0} = (0, \infty)$ denote the time interval required for the data acquisition process and let $\mathbb{R}_T$ be an open interval containing $[0, T]$.

A two-dimensional specimen that changes in time can be described by a time-dependent function $h : \mathbb{R}_T \times \mathbb{R}^2 \to \mathbb{R}$, where $h(t, \cdot)$ corresponds to the state of the searched-for quantity at a fixed time instance $t \in \mathbb{R}_T$. We define $f(x) := h(0, x)$ to be the *initial state* of the specimen. In tomographic applications, the object under investigation typically has compact support at all time instances. Thus, without loss of generality, we assume f (and all object states $h(t, \cdot)$, $t \in \mathbb{R}_T$) to be compactly supported in a fixed open set $\Omega_2 \subset \mathbb{R}^2$.

Let $\Gamma : \mathbb{R}_T \times \Omega_2 \to \Omega_2$ be the mapping which relates the state of the object at time t to its reference configuration f, more precisely

$$h(t, x) = f(\Gamma_t x).$$

Thus, Γ describes the motion of the object particles over time. More precisely, the vector $\Gamma(t, x)$ denotes which particle is at position x at time t.

Throughout the article, we make the following assumption on Γ.

Smooth Diffeomorphic Motion Model
We call a mapping $\Gamma : \mathbb{R}_T \times \Omega_2 \to \Omega_2$ a *smooth diffeomorphic motion model* with *motion functions* $\Gamma_t : \Omega_2 \to \Omega_2$, $\Gamma_t := \Gamma(t, \cdot)$, if the following conditions are satisfied:

- $\Gamma : \mathbb{R}_T \times \Omega_2 \to \Omega_2$ is smooth,
- $\Gamma_t : \Omega_2 \to \Omega_2$ is a diffeomorphism for all $t \in \mathbb{R}_T$.

Remark 1 The diffeomorphism condition guarantees that two particles cannot move into the same position, no particle gets lost (or added) and their relocation is smooth.

In practical applications, only discrete data sets are measured, i.e. the dynamic behavior is only ascertained for finitely many time instances, and the body does move continuously. This justifies the assumption that Γ is smooth with respect to time

3.1 Dynamic FIOs

Let $\mathcal{T}$ be a FIO according to Definition 3 for a static quantity $f \in \mathcal{E}'(\Omega_2)$, where we identify one of the data variables (without loss of generality z_1) as time instance t. Thus, we replace the data variable z by $(t, y) \in \mathbb{R}_T \times \Pi$ where Π is an open subset of $\mathbb{R}$. This results in the representation

$$\mathcal{T} f(t, y) = \int e^{i\Phi(t,y,x,\tau)} a(t, y, x, \tau) f(x) \mathrm{d}x \, \mathrm{d}\tau, \quad (t, y) \in \mathbb{R}_T \times \Pi.$$

In the dynamic setting, at time t, the state of the object $f(\Gamma_t \cdot)$ is encoded by $\mathcal{T}$, resulting (after a change of variables) in the associated dynamic forward operator

$$\mathcal{T}_\Gamma f(t, y) = \int e^{i\Phi(t,y,\Gamma_t^{-1}x,\tau)} a(t, y, \Gamma_t^{-1}x, \tau) \, |\det D_x \Gamma_t^{-1} x| \, f(x) \mathrm{d}x \, \mathrm{d}\tau.$$

We denote

$$a_\Gamma(t, y, x, \tau) := |\det D_x \Gamma_t^{-1} x|\, a(t, y, \Gamma_t^{-1} x, \tau)$$

and

$$\Phi_\Gamma(t, y, x, \tau) := \Phi(t, y, \Gamma_t^{-1} x, \tau)$$

for $(t, y) \in \mathbb{R}_T \times \Pi$, $x \in \Omega_2$, $\tau \in \mathbb{R}^m \setminus \{\mathbf{0}\}$.

Theorem 6 *Let Γ be a smooth diffeomorphic motion model. Assume the static operator $\mathcal{T}$ is a FIO of order $k + (m-2)/2$ (see Definition 3) with amplitude a of order k and non-degenerate phase function Φ. Further, assume*

$$\begin{aligned} &\text{if } (t, y, \Gamma_t^{-1} x, \tau) \in \Sigma_\Phi \text{ and } D_y \Phi = 0, \text{ then} \\ &D_t \Phi(t, y, \Gamma_t^{-1} x, \tau) + D_x \Phi(t, y, \Gamma_t^{-1} x, \tau) \cdot D_t \Gamma_t^{-1} x \neq 0. \end{aligned} \tag{10}$$

Then, $\mathcal{T}_\Gamma$ is a FIO of order $k + (m-2)/2$ with amplitude a_Γ of order k and phase function Φ_Γ. If, in addition, $\mathcal{T}$ is elliptic, then $\mathcal{T}_\Gamma$ is elliptic.

Remark 2 Note that the condition (10) is satisfied if $D_y \Phi$ is never equal to zero on Σ_Φ. We will see in Sect. 3.2 that this is the case for generalized Radon transforms.

Proof Since a is an amplitude of order k, this property transfers to a_Γ due to the smoothness of the motion functions Γ_t and their inverse Γ_t^{-1}.

By the same argument, Φ_Γ inherits the smoothness property from Φ. Since Φ is positive homogeneous of degree 1 in τ, the same holds for Φ_Γ. Thus, Φ_Γ is a phase function.

Using the chain rule, we compute

$$\begin{aligned} D_{(t,y)} \Phi_\Gamma(t, y, x, \tau) &= D_{(t,y)} \Phi(t, y, \Gamma_t^{-1} x, \tau) + D_x \Phi(t, y, \Gamma_t^{-1} x, \tau) \cdot D_{(t,y)} \Gamma_t^{-1} x, \\ D_x \Phi_\Gamma(t, y, x, \tau) &= D_x \Phi(t, y, \Gamma_t^{-1} x, \tau) \cdot D_x \Gamma_t^{-1} x, \end{aligned}$$

and

$$D_\tau \Phi_\Gamma(t, y, x, \tau) = D_\tau \Phi(t, y, \Gamma_t^{-1} x, \tau).$$

From the last property, it follows

$$\begin{aligned} \Sigma_{\Phi_\Gamma} &= \left\{ (t, y, x, \tau) \in \mathbb{R}_T \times \Pi \times \Omega_2 \times \mathbb{R}^m \setminus \{\mathbf{0}\} \;\middle|\; D_\tau \Phi(t, y, \Gamma_t^{-1} x, \tau) = 0 \right\} \\ &= \left\{ (t, y, x, \tau) \;\middle|\; (t, y, \Gamma_t^{-1} x, \tau) \in \Sigma_\Phi \right\}. \end{aligned}$$

Since Φ is non-degenerate, $D_x\Phi$ is nonzero on Σ_Φ. Further, Γ_t^{-1} is a diffeomorphism for all t and therefore, $D_x\Gamma_t^{-1}x$ has nonzero determinant, i.e. the matrix is regular. Thus, on Σ_{Φ_Γ}, the derivative $D_x\Phi_\Gamma(t, y, x, \tau)$ is nonzero. Since $\Gamma_t^{-1}x$ is independent of y, it follows together with condition (10) that Φ_Γ is non-degenerate, and thus, according to Definition 3, $\mathcal{T}_\Gamma$ is a FIO.

The ellipticity of the static FIO $\mathcal{T}$ transfers to its dynamic counterpart $\mathcal{T}_\Gamma$ due to the smoothness of the motion functions Γ_t and inverse Γ_t^{-1} and that Γ_t is a diffeomorphism. □

The next statement follows directly from Theorem 3,

Theorem 7 *Let $\mathcal{T}_\Gamma$ be a FIO (according to Definition 3) with canonical relation C_Γ. Then, for $f \in \mathcal{E}'(\Omega_2)$,*

$$\mathrm{WF}(\mathcal{T}_\Gamma f) \subset C_\Gamma \circ \mathrm{WF}(f).$$

Equality holds if $\mathcal{T}_\gamma$ is elliptic and satisfies the semi-global Bolker Assumption.

Thus, each singularity in the dynamic data stems from a singularity of the object.

Warning
Without additional assumptions on the motion model, the dynamic FIO $\mathcal{T}_\Gamma$ does not, in general, satisfy the semi-global Bolker condition, even if the static FIO $\mathcal{T}$ does. An example corresponds to $\mathcal{T}$ being the classical Radon transform and Γ describing a smooth rotational movement of the same speed than the radiation source, see [18].

In the next section, we state additional assumptions on Γ, under which the semi-global Bolker condition holds at least for dynamic generalized Radon transforms.

3.2 Dynamic Generalized Radon Transforms

The measurement process in many imaging modalities (such as CT, PAT, sonar, etc.) can be modelled by a generalized Radon transform, i.e. an operator that integrates over smooth curves in the plane. We assume the curves are defined as level sets in x of a smooth function $\Psi : \mathbb{R}_T \times \Omega_2 \to \mathbb{R}$. Specifically, we assume the following hypothesis.

Hypothesis 1 Let $\Psi : \mathbb{R}_T \times \Omega_2 \to \mathbb{R}$. If Ψ satisfies the following properties, then Ψ will be called a *defining function*.

1. Ψ is smooth and for all $(t, x) \in \mathbb{R}_T \times \Omega_2$, $D_x\Psi(t, x) \neq \mathbf{0}$.
2. There is an open interval Π such that for each $(t, y) \in \mathbb{R}_t \times \Pi$

$$S(t, y) = \left\{ x \in \Omega_2 \,\middle|\, y = \Psi(t, x) \right\}$$

defines a nontrivial smooth curve.

3. For each $t \in \mathbb{R}_T$, $\Omega_2 \subset \cup_{y \in \Pi} S_\Gamma(t, y)$ (so the curves $S(t, \cdot)$ cover Ω_2).
4. For each compact set $K \subset \Omega_2$, there is a compact subset L of Π such that $K \cap S(t, y) = \emptyset$ for all $(t, y) \in \mathbb{R}_T \times (\Pi \setminus L)$.

Each part of Hypothesis 1 puts more structure on the set of curves $S(t, y)$. Part 1 ensures that each curve is a smooth regular curve. Part 2 means that the curve $S(t, y)$ is defined for all $y \in \Pi$. Part 3 means that, for each t, the curves $S(t, \cdot)$ cover Ω_2, and part 4 will allow us to compose operators in Sect. 4.2 by assuming that $S(t, y)$ is "near" the boundary of Ω_2 if y is "near" the boundary of Π.

With this notation, the generalized Radon transform can be written

$$\mathcal{A}f(t, y) = \int a(t, y, x) f(x) \delta(y - \Psi(t, x)) \, \mathrm{d}x, \quad (t, y) \in \mathbb{R}_T \times \Pi \tag{11}$$

which integrates the quantity f weighted with the C^∞ function a on the curve in $\mathbb{R}^2$ defined by $y = \Psi(t, x)$. Because $D_x \Psi$ is never zero, $\mathcal{A}$ can be written

$$\mathcal{A}f(t, y) = \int e^{i\sigma(y - \Psi(t,x))} a(t, y, x) f(x) \mathrm{d}x \, \mathrm{d}\sigma \tag{12}$$

with phase variable σ in $\mathbb{R}$ and phase $\Phi(t, y, x, \sigma) = \sigma(y - \Psi(t, x))$ and amplitude a. These statements follow from basic facts about the Fourier transform and arguments in [2, 13] and the calculation starting at (10) in [30]. By Theorem 8 below, $\mathcal{A}$ is an FIO.

Due to their practical relevance, we now study this type of operators in more detail.

With a smooth diffeomorphic motion model Γ, the associated dynamic forward operator becomes

$$\mathcal{A}_\Gamma f(t, y) = \int a(t, y, \Gamma_t^{-1} x) f(x) \delta(y - \Psi(t, \Gamma_t^{-1} x)) |\det D_x \Gamma_t^{-1} x| \, \mathrm{d}x \tag{13}$$

for all $(t, y) \in \mathbb{R}_T \times \Pi$. Then, the FIO version is

$$\mathcal{A}_\Gamma f(t, y) = \int e^{i\sigma(y - \Psi(t, \Gamma_t^{-1} x))} a(t, y, \Gamma_t^{-1} x) |\det D_x \Gamma_t^{-1} x| f(x) \, \mathrm{d}x \, \mathrm{d}\sigma. \tag{14}$$

These are justified using a change of variable in (11) and in (12). To simplify the subsequent expressions, we set

$$\Psi_\Gamma(t, x) := \Psi(t, \Gamma_t^{-1} x), \quad (t, x) \in \mathbb{R}_T \times \Omega_2. \tag{15}$$

The operator $\mathcal{A}_\Gamma$ integrates the weighted initial state f along the curves

$$S_\Gamma(t, y) := \left\{ x \in \Omega_2 \,\middle|\, y = \Psi_\Gamma(t, x) \right\}. \tag{16}$$

Our next theorem shows that $\mathcal{A}_\Gamma$ is an elliptic FIO under reasonable conditions.

Theorem 8 *Let Ψ be a defining function, and let $\mathcal{A}$ be the generalized Radon transform defined by (11) where a in (11) is smooth. Then $\mathcal{A}$ is an elliptic FIO of order $-1/2$.*

Let Γ be a smooth diffeomorphic motion model. Then, the dynamic operator $\mathcal{A}_\Gamma$ in (14) is an elliptic FIO of order $-1/2$ with amplitude

$$a_\Gamma(t, y, s, \sigma) = |\det D_x \Gamma_t^{-1} x|\, a(t, y, \Gamma_t^{-1} x),$$

phase function

$$\Phi_\Gamma(t, y, x, \sigma) = \sigma(y - \Psi(t, \Gamma_t^{-1} x)),$$

defining function Φ_Γ and canonical relation

$$C_\Gamma = \left\{ \Big(\big(t, \Psi_\Gamma(t, x)\big), \big(-\sigma\, D_t \Psi_\Gamma(t, x), \sigma \big); x, \sigma\, D_x \Psi_\Gamma(t, x) \Big) \,\middle|\, t \in \mathbb{R}_T, x \in \Omega_2, \sigma \in \mathbb{R} \setminus \{\mathbf{0}\} \right\}.$$

Proof To show that $\mathcal{A}$ is an FIO, we first note that the phase is

$$\Phi(t, y, x, \sigma) = \sigma(y - \Psi(t, x)).$$

Since $D_x \Psi$ is never zero, $D_x \Phi$ is nowhere zero, and $D_y \Phi(t, y, x, \sigma) = \sigma$ is nonzero for all $\sigma \in \mathbb{R} \setminus \{\mathbf{0}\}$, so Φ is a nondegenerate phase function. Therefore, $\mathcal{A}$ satisfies Definition 3 and $\mathcal{A}$ is an FIO. Since a is smooth, positive and independent of σ, a is an amplitude of order zero and so $\mathcal{A}$ is an elliptic FIO of order $-1/2$.

Now, we explain why $\mathcal{A}_\Gamma$ is an elliptic FIO. Since

$$D_y \Phi_\Gamma \Gamma = \sigma \quad \text{and} \quad D_\sigma \Phi_\Gamma(t, y, x, \sigma) = y - \Psi_\Gamma(t, x),$$

the set Σ_{Φ_Γ} is characterized by

$$\Sigma_{\Phi_\Gamma} = \left\{ (t, \Psi_\Gamma(t, x), x, \sigma) \,\middle|\, (t, x, \sigma) \in \mathbb{R}_T \times \Pi \times \Omega_2 \times \mathbb{R} \setminus \{\mathbf{0}\} \right\}.$$

Further, we obtain the derivatives

$$D_x \Phi_\Gamma = -\sigma\, D_x \Psi_\Gamma,$$
$$D_{(t,y)} \Phi_\Gamma = (-\sigma\, D_t \Psi_\Gamma, \sigma).$$

In particular $D_y \Phi_\Gamma \Gamma$ is never equal to zero on Σ_{Φ_Γ}. Thus, $\mathcal{A}_\Gamma$ is an elliptic FIO of order $-1/2$ according to Theorem 6. The stated representation for the canonical relation C_Γ follows directly from the representation of the above derivatives.

The property that Ψ_Γ is a defining function follows from the respective property of Ψ. First, $D_x(\Psi_\Gamma) = D_x \phi D_x \Gamma_t^{-1}$ is nowhere zero by part 1 for Ψ. This proves part 1 for Ψ_Γ. The other parts of the proposition follow from the fact that, for all $t \in \mathbb{R}_T$, $\Gamma_t : \Omega_2 \to \Omega_2$ is a bijective diffeomorphism. □

We now state conditions on the motion model and the phase function such that the dynamic operator $\mathcal{A}_\Gamma$ satisfies the semi-global Bolker assumption.

Theorem 9 *Let Ψ be a defining function, and let $\mathcal{A}$ be the generalized Radon transform defined by* (11) *where a in* (12) *is smooth.*

Let Γ be a smooth diffeomorphic motion model and let $\mathcal{A}_\Gamma$ be the dynamic FIO (13) *with Ψ_Γ given by (15).*

We further assume, that Ψ_Γ satisfies the following additional conditions:

- *The map*

$$x \mapsto \begin{pmatrix} \Psi_\Gamma(t,x) \\ D_t \Psi_\Gamma(t,x) \end{pmatrix} \tag{17}$$

  is one-to-one for each t.
- *For all $x \in \Omega_2$ and all $t \in \mathbb{R}_T$,*

$$\det \begin{pmatrix} D_x \Psi_\Gamma(t,x) \\ D_x D_t \Psi_\Gamma(t,x) \end{pmatrix} \neq 0. \tag{18}$$

Then, $\mathcal{A}_\Gamma$ satisfies the semi-global Bolker Assumption.

Condition (17) implies the injectivity of Π_L, and this ensures that the data, respectively the integration curves, can distinguish different points in the object. Condition (18) implies that $\Pi_L : C_\Gamma \to \mathbb{R}_T \times \Pi \times \mathbb{R}^2 \setminus \{\mathbf{0}\}$ is an immersion (i.e. its derivative is injective), and this guarantees that the integration curves vary sufficiently to detect the object singularities. For a more detailed interpretation, we refer to [18].

The proof has been stated in the literature, for instance in [33] for generic integration curves, in [18] for dynamic CT or in [4] for dynamic PAT. The argument applies by analogy to our case and is therefore omitted here.

Theorem 10 *Let Ψ be a defining function, and let $\mathcal{A}$ be the generalized Radon transform defined by* (11) *where a in* (11) *is smooth. Let Γ be a smooth diffeomorphic motion model. Then, for our dynamic imaging operator $\mathcal{A}_\Gamma$ in* (13)*,*

$$\mathrm{WF}(\mathcal{A}_\Gamma f) \subset C_\Gamma \circ \mathrm{WF}(f).$$

If $\mathcal{A}$ is, in addition, elliptic (a is nowhere zero) and if the motion model satisfies the stronger conditions (17) *and* (18)*, then*

$$\mathrm{WF}(\mathcal{A}_\Gamma f) = C_\Gamma \circ \mathrm{WF}(f).$$

This theorem is a direct consequence of Theorems 7 and 8.

Using the representation of the canonical relation C_Γ from Theorem 8, we obtain the following explicit correspondence between wavefront of $\mathcal{A}_\Gamma f$ and that of f. Let $(t, y) \in \mathbb{R}_T \times \Pi$ and $\sigma \neq 0$, $\nu \in \mathbb{R}$. If $\big((t, y), (-\sigma\nu, \sigma)\big) \in \mathrm{WF}(\mathcal{A}_\Gamma f)$, then there exists an element $x \in S_\Gamma(t, y)$ such that

$$(x, \sigma D_x \Psi_\Gamma(t, x)) \in \mathrm{WF}(f),$$

where $S_\Gamma(t, y)$ is the integration curve given by (16).

If $\mathcal{A}_\Gamma$ is in addition elliptic and satisfies the semi-global Bolker Assumption, then, for $t \in \mathbb{R}_T$, $\big((t, y), (-\sigma\nu, \sigma)\big) \in \mathrm{WF}(\mathcal{A}_\Gamma f)$ if and only if there exists an $x \in S_\Gamma(t, y)$ such that $D_t \Psi_\Gamma(t, x) = \nu$ and $(x, \sigma D_x \Psi_\Gamma(t, x)) \in \mathrm{WF}(f)$. In case such a point x exists, it is unique.

We conclude this section by stating smoothing properties of $\mathcal{A}_\Gamma$ between Sobolev spaces. Note that $\mathbb{R}_T \times \Pi$ is an open subset of $\mathbb{R}^2$ so one can use our definitions for Sobolev spaces on $\mathbb{R}_T \times \Pi$.

Theorem 11 *Let Ψ be a defining function, and let $\mathcal{A}$ be the generalized Radon transform defined by* (11) *where a in* (12) *is smooth. Assume Γ is a smooth diffeomorphic motion model, and assume the dynamic operator $\mathcal{A}_\Gamma$ in* (13) *satisfies the additional condition (18). Then,*

$$\mathcal{A}_\Gamma : H_c^s(\Omega_2) \to H_{loc}^{s+1/2}(\mathbb{R}_T \times \Pi)$$

is continuous.

Proof According to Theorem 8, $\mathcal{A}_\Gamma$ is a FIO of order $k = -1/2$. Additionally, condition (18) yields that the projection $\Pi_L : C_\Gamma \to T^*(\mathbb{R}_T \times \Pi) \setminus \{\mathbf{0}\}$ is an immersion. Hence, we can apply Theorem 5 and obtain that $\mathcal{A}_\Gamma : H_c^s(\Omega_2) \to H_{loc}^{s+1/2}(\mathbb{R}_T \times \Pi)$ is continuous. □

According to the above theorem, the data $\mathcal{A}_\Gamma f$ are smoother than f by 1/2 in Sobolev scale. In particular, for a smooth diffeomorphic motion model satisfying (17) and (18), $\mathcal{A}_\Gamma$ has the same smoothing property as the static operator $\mathcal{A}$.

After analyzing the overall information content of dynamic data, we now study which object singularities can be reliably reconstructed and which additional artifacts have to be expected.

4 Reconstruction Operators and Artefact Study

In this section, we apply the theory of microlocal analysis to define and analyze reconstruction operators to solve dynamic inverse problems $\mathcal{T}_\Gamma f = g$. From Sect. 2, we know that Fourier integral operators encode singularities of f in specific ways. The idea now is to construct reconstruction operators which recover the visible singularities from the measured data $g = \mathcal{T}_\Gamma f$.

4.1 An Ideal Scenario: Smoothly Periodic Motion

In practical applications, data can only be measured for t in a closed interval $[0, T] \subset \mathbb{R}_T$. From a theoretical point of view, this is troublesome since smooth function (and hence distributions) are defined on open sets in order for derivatives to be well defined.

For a specific type of functions, namely smoothly T-periodic functions, this does not impose a restriction. A function of t (and perhaps other variables) will be called *smoothly $T-$periodic* if it extends to $t \in \mathbb{R}$ as a smooth function that is $T-$periodic. This allows us to define $\mathcal{E}([0, T] \times \Pi)$ to be the set of functions on $[0, T] \times \Pi$ which extend to functions on $\mathbb{R} \times \Pi$ that are smooth and $T-$periodic in t. The set $\mathcal{D}([0, T] \times \Pi)$ then denotes the set of those functions with compact support.

We start our study of reconstruction operators within this idealized framework by assuming that the motion model Γ, the amplitude a and the phase function Φ (and Ψ in case of a generalized Radon transform) are all smoothly $T-$periodic. So, for example, Γ can be extended in t to a function on $\mathbb{R}$ and $\Gamma(t, \cdot) = \Gamma(t + T, \cdot)$ for all $t \in \mathbb{R}$.

The dual operator plays a crucial role, and it is defined by

$$\mathcal{T}_\Gamma^t g(x) = \int_{[0,T]} \int_\Pi \int_{\mathbb{R}^2} e^{i\Phi(t,y,\Gamma_t^{-1}x,\tau)} a(t, y, \Gamma_t^{-1}x, \tau) \,|\det D_x \Gamma_t^{-1} x|\, g(t, y)\, \mathrm{d}\tau\, \mathrm{d}y\, \mathrm{d}t.$$

In particular, the operator $\mathcal{T}_\Gamma^t$ then corresponds to the formal dual of $\mathcal{T}_\Gamma$ for $g \in \mathcal{D}([0, T] \times \Pi)$.

For dynamic generalized Radon transforms as in (13), this corresponds to the *backprojection operator* $\mathcal{A}_\Gamma^t$ defined by

$$\mathcal{A}_\Gamma^t g(x) = \int_{t\in[0,T]} a_\Gamma(t, \Psi_\Gamma(t, x), x) g(t, \Psi_\Gamma(t, x)) \mathrm{d}t, \tag{19}$$

for $g \in \mathcal{E}(\mathbb{R}_T \times \Pi)$. This is true by taking the expression (13) and calculating its dual and integrating the δ function with respect to y.

Our next theorem provides conditions under which $\mathcal{T}_\Gamma$ is an FIO in the $T-$periodic case, and this includes dynamic generalized Radon transforms satisfying Hypothesis 1.

Theorem 12 *Let Γ be a smooth diffeomorphic $T-$periodic motion model such that $\mathcal{T}_\Gamma$ is a dynamic FIO that satisfies the semi-global Bolker Assumption. In addition, assume that $\mathcal{T}_\Gamma$ and ${\mathcal{T}_\Gamma}^t$ are both strongly continuous as mappings*

$$\mathcal{T}_\Gamma : \mathcal{D}(\Omega_2) \to \mathcal{D}([0,T] \times \Pi), \quad \mathcal{T}_\Gamma^t : \mathcal{E}([0,T] \times \Pi) \to \mathcal{E}(\Omega_2). \tag{20}$$

Let $\mathcal{P}$ be a PSIDO. Then, the operator

$$\mathcal{L}_\Gamma := \mathcal{T}_\Gamma^t \mathcal{P} \mathcal{T}_\Gamma$$

is well defined for $f \in \mathcal{E}'(\Omega_2)$ and

$$\mathrm{WF}(\mathcal{L}_\Gamma f) \subset \mathrm{WF}(f). \tag{21}$$

Now, assume that $\mathcal{P}$ and $\mathcal{T}_\Gamma$ are elliptic with positive symbols and the natural projection $\Pi_R : C_\Gamma \to \Omega_2 \times \mathbb{R}^2 \setminus \{\mathbf{0}\}$ is surjective. Then

$$\mathrm{WF}(\mathcal{L}_\Gamma f) = \mathrm{WF}(f). \tag{22}$$

Let Ψ be smoothly $T-$periodic and satisfy Hypothesis 1 and let $\mathcal{A}$ be a generalized Radon transform with defining function Ψ. Then (20) holds for $\mathcal{A}_\Gamma$. Therefore, (21) and (22) hold under the appropriate hypotheses above.

Proof Let C_Γ denote the canonical relation of the FIO $\mathcal{T}_\Gamma$. Since, the operator $\mathcal{T}_\Gamma^t$ is the formal dual of $\mathcal{T}_\Gamma$, it is a FIO as well with canonical relation C_Γ^t. As $\mathcal{T}_\Gamma$ satisfies the semi-global Bolker Assumption,

$$C_\Gamma^t \circ C_\Gamma \subset \Delta := \left\{ (x,\xi;x,\xi) \,\middle|\, (x,\xi) \in \Omega_2 \times \mathbb{R}^2 \setminus \{\mathbf{0}\} \right\}.$$

According to Theorem 4, the PSIDO $\mathcal{P} : \mathcal{E}'([0,T] \times \Pi) \to \mathcal{D}'([0,T] \times \Pi)$ is weakly continuous. By duality with their adjoints and the continuity assumptions (20), $\mathcal{T}_\Gamma : \mathcal{E}'(\mathbb{R}^2) \to \mathcal{E}'([0,T] \times \Pi)$ is weakly continuous as is $\mathcal{T}_\Gamma^t : \mathcal{D}'([0,T] \times \Pi) \to \mathcal{D}'(\Omega_2)$. Therefore, the composition $\mathcal{L}_\Gamma := \mathcal{T}_\Gamma^t \mathcal{P} \mathcal{T}_\Gamma$ is well-defined and weakly continuous for $f \in \mathcal{E}'(\Omega_2)$.

Using Theorem 3, we obtain

$$\mathrm{WF}(\mathcal{L}_\Gamma f) \subset C_\Gamma^t \circ C_\Gamma \circ \mathrm{WF}(f) \subset \mathrm{WF}(f).$$

Next we explain why equality holds in (21) if all operators are elliptic, $\mathcal{T}_\Gamma$ satisfies the semi-global Bolker Assumption and Π_R is surjective from C_Γ to $\Omega_2 \times \mathbb{R}^2 \setminus \{\mathbf{0}\}$. Since $\mathcal{P}$ is a PSIDO, its canonical relation is Δ. Since Π_R is surjective, $C_\Gamma^t \circ \Delta \circ C_\Gamma = \Delta$. By the semi-global Bolker Assumption, the operators can be

composed as FIO, and since they are all elliptic the symbol of the composition, $\mathcal{L}_\Gamma$, is the product symbol on the product canonical relations pulled back to Δ (see the symbol calculation in [30]). In this case, $\mathcal{L}_\Gamma$ is an elliptic PSIDO and equality holds in (21).

Now let $\mathcal{A}$ be a $T-$periodic generalized Radon transform with defining function, Ψ. Since Ψ satisfies Hypothesis 1, the dynamic generalized Radon transform $\mathcal{A}_\Gamma$ is a $T-$periodic FIO with defining function Ψ_Γ.

We now outline the proof of (20) for $\mathcal{A}_\Gamma$. Let K be a compact subset of Ω_2 and let $L \subset \Pi$ be the compact set in Hypothesis 1 part 4 for K. Then, $\mathcal{A}_\Gamma$ maps functions supported in K to functions supported in $[0, T] \times L$. One proves that this map is continuous from $\mathcal{D}_K$ to $\mathcal{D}_{[0,T]\times L}$ (see [35, sections 6.1-6.6]) using the explicit expression (13) (or that $\mathcal{A}_\Gamma$ is a generalized Radon transform, e.g., [30]). To prove that $\mathcal{A}_\Gamma^t : \mathcal{E}([0, T] \times \Pi) \to \mathcal{E}(\Omega_2)$, one uses the expression (19) for $\mathcal{A}_\Gamma^t$ and the fact that $[0, T]$ is compact and all functions are smoothly $T-$periodic. This allows us to apply the statements for $\mathcal{T}_\Gamma$ for $\mathcal{A}_\Gamma$. □

Theorem 12 provides a strategy to design suitable reconstruction operators. If we choose a PSIDO as above, then the operator

$$\mathcal{S}_\Gamma := \mathcal{T}_\Gamma^t \mathcal{P}$$

applied to the data $g = \mathcal{T}_\Gamma f$ provides an image $\mathcal{L}_\Gamma f$ whose singularities coincide with singularities of the searched-for quantity f. In particular, $\mathcal{L}_\Gamma f$ displays the object singularities that it reconstructs at their correct location with the correct direction, i.e. the motion is compensated for. If the operators are elliptic and the other assumptions of Theorem 12 hold, then $\mathcal{L}_\Gamma f$ reproduces all singularities of f. Therefore, $\mathcal{L}_\Gamma f = \mathcal{T}_\Gamma^t \mathcal{P} \mathcal{T}_\Gamma f = \mathcal{S}_\Gamma g$ can be interpreted as an approximate inversion formula for the purpose of motion compensation.

4.2 The Realistic Case: Non-periodic Motion

The T-periodicity assumption on Γ in the last section imposes a severe restriction regarding practical applications. This assumption implies that the data have to encode the same state of the object at beginning and end of the scanning–a condition which, in general, will not be met.

Therefore, we want to analyze this more realistic setting in the following. More generally, we consider the scenario that data $g(t, y) = \mathcal{T}_\Gamma f(t, y)$ are measured for $(t, y) \in [\alpha, \beta] \subset \mathbb{R}_T$ with $0 \leq \alpha < \beta \leq T$. This framework covers, for instance, also data acquisition protocols with limited angular range. Then, formally, the forward operator $\mathcal{T}_\Gamma$ needs to be restricted to the data set. This can be achieved by multiplying with the characteristic function $\chi_{[\alpha,\beta]\times\Pi}$ of $[\alpha, \beta] \times \Pi$.

In order to study the effect on the singularities in the data and under reconstruction, we can apply the paradigm given in [10] which characterizes a broad range of incomplete data problems. In particular, the study divides into the following steps:

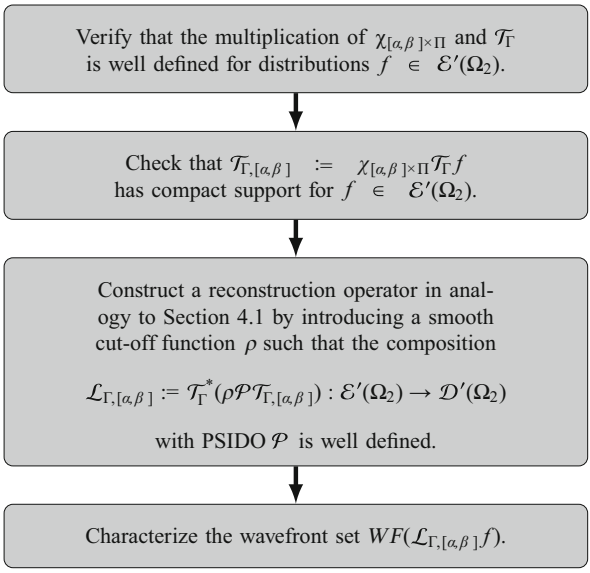

Note if ${\mathcal{T}_\Gamma}^* : \mathcal{D}' \to \mathcal{D}'$ then the cutoff ρ is not necessary.

With this general outline, we now perform the artefact study for operator $\mathcal{A}_\Gamma$ from Sect. 3.2 (13), i.e. for a dynamic generalized Radon transform with smooth diffeomorphic motion model Γ.

First, we verify that the multiplication with the characteristic function $\chi_{[\alpha,\beta]\times\Pi}$ is well-defined.

Proposition 1 *Assume Ψ satisfies Hypothesis 1 and Γ is a smooth motion model. Then, the operator $\mathcal{A}_{\Gamma,[\alpha,\beta]}f := \chi_{[\alpha,\beta]\times\Pi}\mathcal{A}_\Gamma f$ is well-defined for distributions $f \in \mathcal{E}'(\Omega_2)$.*

Proof Let $f \in \mathcal{E}'(\Omega_2)$. We apply Theorem 1 with the data set $B := [\alpha, \beta] \times \Pi$. Using the representation of the canonical relation C_Γ of $\mathcal{A}_\Gamma$ (see Theorem 8), it follows that

$$C_\Gamma \circ \mathrm{WF}(f) \subset \left\{(t, y, \xi) \in \mathbb{R}_T \times \Pi \times \mathbb{R}^2 \setminus \{\mathbf{0}\} \,\middle|\, \xi_2 \neq 0\right\}. \tag{23}$$

However, $\mathrm{WF}(\chi_{[\alpha,\beta]}) = \left\{(t, y, \xi_1, 0) \,\middle|\, t \in \{\alpha, \beta\}, y \in \Pi, \xi_1 \neq 0\right\}$. Therefore sums of such points are of the form (t, y, η_1, ξ_2) where $\xi_2 \neq 0$. Therefore, the non-cancellation condition (2) holds, and Theorem 1 can be used to conclude that $\mathcal{A}_{\Gamma,[\alpha,\beta]}f$ is well-defined for $f \in \mathcal{E}'(\Omega_2)$. □

Proposition 2 *Assume* Ψ *satisfies Hypothesis 1 and* Γ *is a smooth motion model. Then,* $\mathcal{A}_{\Gamma,[\alpha,\beta]}f$ *has compact support for all* $f \in \mathcal{E}'(\Omega_2)$*, i.e.* $\mathcal{A}_{\Gamma,[\alpha,\beta]} : \mathcal{E}'(\Omega_2) \to \mathcal{E}'(\mathbb{R}_T \times \Pi)$.

Proof Let $f \in \mathcal{E}'(\Omega_2)$. By Theorem 8, Ψ_Γ is a defining function. Thus, according to Hypothesis 1 part 4, there is a compact set $L \subset \Pi$ such that $\mathcal{A}_\Gamma f(t, y)$ is supported on $\mathbb{R}_T \times L$.

Because $\chi_{[\alpha,\beta]}$ is zero for $t \notin [\alpha, \beta]$ and all y and $\mathcal{A}_{\Gamma,[\alpha,\beta]}f$ is zero for all y outside a compact set, the product, $\mathcal{A}_{\Gamma,[\alpha,\beta]}f$ has compact support in $[\alpha, \beta] \times L$. □

The formal dual to $\mathcal{A}_\Gamma$ on $\mathbb{R}_T \times \Pi$ is given by

$$\mathcal{A}_\Gamma^* g(x) = \int_{\mathbb{R}_T} a_\Gamma(t, \Psi_\Gamma(t, x), x)\ g(t, \Psi_\Gamma(t, x))\mathrm{d}t. \tag{24}$$

Since the domain of $\mathcal{A}_\Gamma^*$ is not, in general, $\mathcal{D}'(\mathbb{R}_T \times \Pi)$, we multiply by a smooth cutoff function. Therefore, let $\rho : \mathbb{R}_T \to \mathbb{R}$ be smooth and equal to one on $[\alpha, \beta]$ and be supported in $\mathbb{R}_T$. The corresponding restricted backprojection operator is then given by

$$\mathcal{A}_{\Gamma,\rho}^t g := \mathcal{A}_\Gamma^*(\rho g). \tag{25}$$

In analogy to Sect. 4.1, we would like to consider

$$\mathcal{L}_{\Gamma,[\alpha,\beta]} := \mathcal{A}_{\Gamma,\rho}^t \mathcal{P} \mathcal{A}_{\Gamma,[\alpha,\beta]}, \tag{26}$$

with a PSIDO $\mathcal{P}$ to build a reconstruction operator for the non-periodic case. Therefore, we have to prove that this composition is well-defined.

Proposition 3 *Let* $\mathcal{P}$ *be a pseudodifferential operator, then* $\mathcal{A}_{\Gamma,\rho}^t$*,* $\mathcal{P}$*, and* $\mathcal{A}_{\Gamma,[\alpha,\beta]}$ *can be composed and* $\mathcal{L}_{\Gamma,[\alpha,\beta]} : \mathcal{E}'(\Omega_2) \to \mathcal{D}'(\Omega_2)$ *is well-defined.*

Proof From Propositions 1 and 2, we know that $\mathcal{A}_{\Gamma,[\alpha,\beta]}f \in \mathcal{E}'(\mathbb{R}_T \times \Pi)$ for $f \in \mathcal{E}'(\Omega_2)$. Therefore, $\mathcal{P}\mathcal{A}_{\Gamma,[\alpha,\beta]}f$ is defined as a distribution in $\mathcal{D}'(\mathbb{R}_T \times \Pi)$.

Since $\mathcal{M}_\rho : g \mapsto \mathcal{M}_\rho := \rho g$ is a trivial pseudodifferential operator, which is continuous on $\mathcal{D}(\mathbb{R}_T \times \Pi)$, the operator $\mathcal{M}_\rho \mathcal{A}_\Gamma = \rho \mathcal{A}_\Gamma$ is continuous from $\mathcal{D}(\Omega_2)$ to $\mathcal{D}(\mathbb{R}_T \times \Pi)$. Here we use Hypothesis 1 and the fact that ρ has compact support in t.

This implies, that the dual $(\mathcal{M}_\rho \mathcal{A}_\Gamma)^* = (\rho \mathcal{A}_\Gamma)^* = \mathcal{A}_\Gamma^* \rho = \mathcal{A}_{\Gamma,\rho}^t$ is weakly continuous from $\mathcal{D}'(\mathbb{R}_T \times \Pi)$ to $\mathcal{D}'(\Omega_2)$. Therefore, $\mathcal{L}_{\Gamma,[\alpha,\beta]}$ is well-defined. □

We now state the main result of this section, which provides a characterization of the visible singularities and the possible added artifacts from data above $[\alpha, \beta]$.

Theorem 13 *Let* $f \in \mathcal{E}'(\Omega_2)$ *and* Γ *be a smooth diffeomorphic motion which satisfies the additional conditions (17) and (18). Further, let* $\mathcal{P}$ *be a PSIDO and*

$\mathcal{L}_{\Gamma,[\alpha,\beta]}$ be given by (26) where Ψ satisfies Hypothesis 1. Then,

$$\mathrm{WF}(\mathcal{L}_{\Gamma,[\alpha,\beta]} f) \subset (\mathrm{WF}(f) \cap \mathcal{V}_{[\alpha,\beta]}) \cup \mathcal{Z}_{\{\alpha,\beta\}}(f),$$

where

$$\mathcal{V}_{[\alpha,\beta]} := \left\{(x, \sigma \partial_x \Psi_\Gamma(t,x)) \,\middle|\, x \in \Omega_2,\ t \in [\alpha,\beta],\ \sigma \in \mathbb{R} \setminus \{\mathbf{0}\}\right\}$$

is the set of all (potentially) visible singularities from data above $[\alpha, \beta]$, and

$$\mathcal{Z}_{\{\alpha,\beta\}}(f) := \left\{(x, \sigma D_x \Psi_\Gamma(t,x)) \,\middle|\, t \in \{\alpha,\beta\},\ y \in \Pi,\ x \in \mathcal{S}_\Gamma(t,y),\ \sigma \in \mathbb{R} \setminus \{\mathbf{0}\},\ \exists \tilde{x} \in \mathcal{S}_\Gamma(t,y) :\ (\tilde{x}, \sigma D_x \Psi_\Gamma(t,\tilde{x})) \in \mathrm{WF}(f)\right\}$$

denotes the set of (possible) added artifacts.

Proof Since ρ is a smooth cutoff, $\mathcal{A}^t_{\Gamma,\rho}$ is a FIO with the same canonical relation as $\mathcal{A}^*_\Gamma$. Thus, we have

$$\mathrm{WF}(\mathcal{L}_{\Gamma,[\alpha,\beta]} f) = \mathrm{WF}(\mathcal{A}^t_{\Gamma,\Phi} \mathcal{P} \mathcal{A}_{\Gamma,[\alpha,\beta]} f) \subset C^t_\Gamma \circ \mathrm{WF}(\mathcal{P}\mathcal{A}_{\Gamma,[\alpha,\beta]} f). \tag{27}$$

Further, $\mathcal{P}$ is a pseudodifferential operator, i.e. its canonical relation is Δ and therefore

$$\mathrm{WF}(\mathcal{P}\mathcal{A}_{\Gamma,[\alpha,\beta]} f) \subset \mathrm{WF}(\mathcal{A}_{\Gamma,[\alpha,\beta]} f).$$

Following Proposition 1 and Theorem 1, we obtain

$$\mathrm{WF}(\mathcal{A}_{\Gamma,[\alpha,\beta]} f) \subset Q([\alpha,\beta] \times \Pi, \mathrm{WF}(\mathcal{A}_\Gamma f)) \tag{28}$$

with Q defined in Theorem 1. From Theorem 10, we know $\mathrm{WF}(\mathcal{A}_\Gamma f) \subset C_\Gamma \circ \mathrm{WF}(f)$ and hence

$$\mathrm{WF}(\mathcal{L}_{\Gamma,[\alpha,\beta]} f) \subset C^t_\Gamma \circ Q([\alpha,\beta] \times \Pi, C_\Gamma \circ \mathrm{WF}(f)). \tag{29}$$

From the definition, we get

$$\begin{aligned} &Q([\alpha,\beta] \times \Pi, C_\Gamma \circ \mathrm{WF}(f)) \\ &= \left\{(z, \xi + \eta) \,\middle|\, z \in [\alpha,\beta] \times \Pi, [(z,\xi) \in C_\Gamma \circ \mathrm{WF}(f) \vee \xi = 0] \right. \\ &\qquad \left. \wedge\, [(z,\eta) \in \mathrm{WF}(\chi_{[\alpha,\beta]\times\Pi}) \vee \eta = 0]\right\}. \end{aligned}$$

This set can be written as a union of three sets

$$Q([\alpha,\beta] \times \Pi, C_\Gamma \circ \mathrm{WF}(f)) = (C_\Gamma \circ \mathrm{WF}(f)) \cap ([\alpha,\beta] \times \Pi \times \mathbb{R}^2 \setminus \{\mathbf{0}\})$$

$$\cup\, \mathrm{WF}(\chi_{[\alpha,\beta]\times\Pi})$$
$$\cup\, \mathcal{W}_{\{\alpha,\beta\}}(f),$$

where $\mathcal{W}_{\{\alpha,\beta\}}(f)$ summarizes the case $\xi \neq 0 \wedge \eta \neq 0$, i.e. the set is defined by

$$\begin{aligned}\mathcal{W}_{\{\alpha,\beta\}}(f) &:= \big\{(z, \xi+\eta)\,\big|\\ &\qquad z \in [\alpha,\beta]\times\Pi,\ (z,\xi)\in C_\Gamma \circ \mathrm{WF}(f),\ (z,\eta)\in \mathrm{WF}(\chi_{[\alpha,\beta]\times\Pi})\big\}\\ &= \big\{((t,y),(\nu,\sigma)\,\big|\, t\in\{\alpha,\beta\},\ \nu\in\mathbb{R},\ y\in\Pi,\ \sigma\in\mathbb{R}\setminus\{\mathbf{0}\},\\ &\qquad \exists x\in\mathcal{S}_\Gamma(t,y):\ (x,\sigma D_x\Psi_\Gamma(t,x))\in \mathrm{WF}(f)\big\}.\end{aligned}$$

Hence, we obtain

$$\mathrm{WF}(\mathcal{L}_{\Gamma,[\alpha,\beta]}f) \subset C_\Gamma^t \circ \big[(C_\Gamma\circ\mathrm{WF}(f))\cap([\alpha,\beta]\times\Pi\times\mathbb{R}^2\setminus\{\mathbf{0}\})\big] \tag{30}$$
$$\cup\, C_\Gamma^t\circ \mathrm{WF}(\chi_{[\alpha,\beta]\times\Pi}) \tag{31}$$
$$\cup\, C_\Gamma^t\circ \mathcal{W}_{\{\alpha,\beta\}}(f). \tag{32}$$

Under the additional conditions (17) and (18) on the motion Γ, $\mathcal{A}_\Gamma$ satisfies the semi-global Bolker Assumption (see Theorem 9). Thus, $C_\Gamma^t\circ C_\Gamma \subset \Delta$ and $C_\Gamma^t\circ C_\Gamma\circ\mathrm{WF}(f)\subset \mathrm{WF}(f)$.

Therefore, the first component (30) yields

$$\begin{aligned}C_\Gamma^t\circ\big[(C_\Gamma\circ\mathrm{WF}(f))\cap([\alpha,\beta]\times\Pi\times\mathbb{R}^2\setminus\{\mathbf{0}\})\big]&\\ \subset \mathrm{WF}(f)\cap(C_\Gamma^t\circ([\alpha,\beta]\times\Pi\times\mathbb{R}^2\setminus\{\mathbf{0}\})).&\end{aligned}$$

Since

$$\begin{aligned}C_\Gamma^t = \big\{(x,\sigma D_x\Psi_\Gamma(t,x);\,(t,\Psi_\Gamma(t,x)),(-\sigma\partial_t\Psi_\Gamma(t,x),\sigma))\,\big|&\\ t\in[\alpha,\beta],\ x\in\Omega_2,\ \sigma\in\mathbb{R}\setminus\{\mathbf{0}\}\big\}&\end{aligned}$$

we obtain

$$\begin{aligned}C_\Gamma^t\circ([\alpha,\beta]\times\Pi\times\mathbb{R}^2\setminus\{\mathbf{0}\}) &= \big\{(x,\sigma D_x\Psi_\Gamma(t,x))\,\big|\, t\in[\alpha,\beta],\ x\in\Omega_2,\ \sigma\in\mathbb{R}\setminus\{\mathbf{0}\}\big\}\\ &= \mathcal{V}_{[\alpha,\beta]}.\end{aligned}$$

For the second component (31), we have $C_\Gamma^t\circ\mathrm{WF}(\chi_{[\alpha,\beta]\times\Pi})=\emptyset$, since for any $(x,\xi)\in\mathrm{WF}(\chi_{[\alpha,\beta]\times\Pi})$ it is $\xi_2=0$, but for all vectors $((z,\eta),(\tilde{x},\tilde{\xi}))\in C_\Gamma^t$ we have $\tilde{\xi}_2=\sigma\neq 0$.

Now, we consider the third set (32): $C_\Gamma^t\circ\mathcal{W}_{\{\alpha,\beta\}}(f)$.

Let $\rho = ((t, y), (\nu, \sigma)) \in \mathcal{W}_{\{\alpha,\beta\}}(f)$. Then, we obtain from the definition of the set $\mathcal{W}_{\{\alpha,\beta\}}(f)$, that $t \in \{\alpha, \beta\}$, $\nu \in \mathbb{R}$, $y \in \Pi$, $\sigma \in \mathbb{R} \setminus \{\mathbf{0}\}$ and that there exists an element $x \in \mathcal{S}_\Gamma(t, y)$ with $(x, \sigma D_x \Psi_\Gamma(t, x)) \in \mathrm{WF}(f)$. So any element of the set

$$C_\Gamma^t \circ \{\rho\} = \left\{ (\tilde{x}, \sigma D_x \Psi_\Gamma(t, \tilde{x})) \,\middle|\, (\tilde{x}, \sigma D_x \Psi_\Gamma(t, \tilde{x}), \rho) \in C_\Gamma^t \right\} \tag{33}$$

has to fulfill $s = \Psi_\Gamma(t, \tilde{x})$ (by definition of C_Γ^t) and

$$\nu = -\sigma \mathrm{D}_t \Psi_\Gamma(t, \tilde{x}) \;\Leftrightarrow\; -\frac{\nu}{\sigma} = \mathrm{D}_t \Psi_\Gamma(t, \tilde{x}).$$

Since ν is arbitrary, the set (33) is nonempty. Hence, for any $\tilde{x} \in \mathcal{S}_\Gamma(t, y)$, we have $(\tilde{x}, \sigma D_x \Psi_\Gamma(t, \tilde{x})) \in C_\Gamma^t \circ \mathcal{W}_{\{\alpha,\beta\}}(f)$ and

$$\begin{aligned} C_\Gamma^t \circ \mathcal{W}_{\{\alpha,\beta\}}(f) = \Big\{ (\tilde{x}, \sigma D_x \Psi_\Gamma(t, \tilde{x})) \,\Big|\, & t \in \{\alpha, \beta\},\, y \in \Pi,\, \tilde{x} \in \mathcal{S}_\Gamma(t, y),\, \sigma \in \mathbb{R} \setminus \{\mathbf{0}\}, \\ & \exists x \in \mathcal{S}_\Gamma(t, y) :\; (x, \sigma D_x \Psi_\Gamma(t, x)) \in \mathrm{WF}(f) \Big\} \\ = \mathcal{Z}_{\{\alpha,\beta\}}(f). \end{aligned}$$

This concludes the proof. □

The above theorem shows that only singularities, which are in the visibility range (i.e., in $\mathcal{V}_{[\alpha,\beta]}$) can be reconstructed from the dynamic data, whereas singularities outside of this range are smoothed. According to the computations within the proof, the singularities arising in a reconstruction $\mathcal{L}_\Gamma f$ can be divided into three categories:

- Visible singularities of f from data above $[\alpha, \beta]$
  (corresponding to the set $\mathrm{WF}_{[\alpha,\beta]}(f)$),
- Added artefacts that stem from the scanning geometry and that are independent of the object f
  (corresponding to the set $C_\Gamma^t \circ \mathrm{WF}(\chi_{[\alpha,\beta]\times\Pi})$),
- Added artefacts that stem from the object
  (corresponding to the set $\mathcal{Z}_{\Gamma,[\alpha,\beta]}$).

The proof further reveals that the artefact set $C_\Gamma^t \circ \mathrm{WF}(\chi_{[\alpha,\beta]\times\Pi})$ is empty in our case of generalized Radon transforms. However, for different cutoff functions than $\chi_{[\alpha,\beta]\times\Pi}$, this might no longer be the case, see [3].

The added artefacts stemming from the object can be descriptively characterized as follows. If $(x, \sigma \partial_x \Psi_\Gamma(t_0, x)) \in \mathrm{WF}(f)$, where $t_0 \in \{\alpha, \beta\}$, then this singularity of f can generate artifacts along the curve $\mathcal{S}_\Gamma(t_0, \Psi_\Gamma(t_0, x))$.

In the next section we illustrate this theoretical characterization by numerical examples.

5 Numerical Results

In this section, we want to illustrate our theoretical results at numerical examples from Photoacoustic tomography (PAT).

In this imaging modality, an organism is subjected to non-ionizing laser pulses. The biological tissue absorbs a part of the delivered energy and converts it into heat generating ultrasonic pressure waves (photoacoustic effect). The emitted waves propagate through the medium and are measured by transducers located outside the organism on an observation surface. The goal is to recover the initial pressure $f(x)$ from the measured response g since it encodes characteristic information about the biological tissue.

In practical PAT applications, the object is not entirely surrounded by transducers. We consider the case where the transducer rotates around the object, thus acquiring the data g sequentially in time [4, 17].

Under simplifying assumptions, the measured data g match in the two-dimensional setting with the circular Radon transform of the initial pressure $f(x)$, i.e.

$$g(t, y) = \frac{1}{2\pi y} \int f(x)\, \delta(y - \|\theta(t) - x\|)\, \mathrm{d}x =: \mathcal{A} f(t, y),$$

for $f \in \mathcal{E}'(V_1(0))$, $V_1(0)$ being the open unit disk and where $(t, y) \in [0, 2\pi] \times (0, 2)$ and $\theta(t) = (\cos t, \sin t)^T$. In particular $\mathcal{A}$ represents a FIO with amplitude $a(y) = (2\pi y)^{-1}$ and phase function $\Phi(t, y, x, \sigma) = \sigma(y - \Psi(t, y, x))$, where $\Psi(t, y, x) = \|\theta(t) - x\|$ is a defining function according to our Hypothesis 1.

If the searched-for quantity changes during the sequential data acquisition according to a smooth diffeomorphic motion model Γ, the corresponding dynamic forward operator

$$\mathcal{A}_\Gamma f(t, y) = \frac{1}{2\pi y} \int f(x)\, |\det D\Gamma_t^{-1} x|\, \delta(y - \|\theta(t) - \Gamma_t^{-1} x\|)\, \mathrm{d}x \tag{34}$$

is a FIO according to Theorem 8 which integrates the reference configuration $f(x)$ along the curves

$$S_\Gamma(t, y) := \{x \in V_1(0) \,\big|\, y = \Psi_\Gamma(t, x)\}$$

with

$$\Psi_\Gamma(t, x) = \|\theta(t) - \Gamma_t^{-1} x\|. \tag{35}$$

If the motion model fulfills the additional conditions (17) and (18), then $\mathcal{A}_\Gamma$ satisfies the semi-global Bolker Assumption.

In particular, we want to illustrate the reconstruction results obtained by applying an operator of type

$$\mathcal{S}_\Gamma := \mathcal{A}^t_{\Gamma,[0,2\pi]}\mathcal{P}$$

to the dynamic data $g(t, y) = \mathcal{A}_\Gamma f(t, y)$, $(t, y) \in [0, 2\pi] \times (0, 2)$ with

$$\mathcal{P}g(t, y) = \int \partial_r r \partial_r g(t, r) \log|r^2 - y^2| \, \mathrm{d}r$$

stemming from the inversion formula for $\mathcal{A}$ in the static case, see [7, 17]. In the following examples, we simulate (dynamic) PAT data by discretizing $\mathcal{A}_\Gamma f$ with the trapezoidal rule with 1400 samples, where f is the respective phantom. The discrete dynamic data is then given by

$$g_{i,j} := (\mathcal{A}_{\Gamma_{t_i}} f)(t_i, y_j), \quad i = 1, \ldots, N \text{ and } j = 1, \ldots, M,$$

with $N = 300$ uniformly distributed angles t_i in $[0, 2\pi]$ and $M = 300$ uniformly distributed radii y_j in $(0, 2]$. The reconstructed images are computed on a 600×600 grid.

5.1 2π-Periodic Motion

For our first numerical example, we consider the ideal scenario (from Sect. 4.1), where we have a smooth and 2π-periodic motion model. More precisely, we consider the rotation matrix

$$B_t = \begin{pmatrix} \cos(2t) & \sin(2t) \\ -\sin(2t) & \cos(2t) \end{pmatrix},$$

which defines a 2π-periodic motion $\Gamma_t x = B_t x$ for $x \in \mathbb{R}^2$ and $t \in [0, 2\pi]$. The dynamic behavior of the object–namely a rotation in the same direction as the transducer but twice as fast–is illustrated in Fig. 4. In particular, with Γ describing such a rotational movement, the representation (34) of the dynamic FIO $\mathcal{A}_\Gamma$ simplifies to

$$\mathcal{A}_\Gamma f(t, y) = \frac{1}{2\pi y} \int f(x) \, \delta(y - \|B_t \theta(t) - x\|) \, \mathrm{d}x,$$

i.e. the dynamic behavior of f can be equivalently expressed by adapting the rotation of the transducer, see [16] for more details.

From our theory (in particular Theorem 12), we expect to see no additional artefacts and, since all singularities are encoded in the data according to the theory developed in Sect. 3, we anticipate to see all singularities correctly reconstructed. These theoretical results are indeed confirmed by our numerical reconstruction result in Fig. 5.

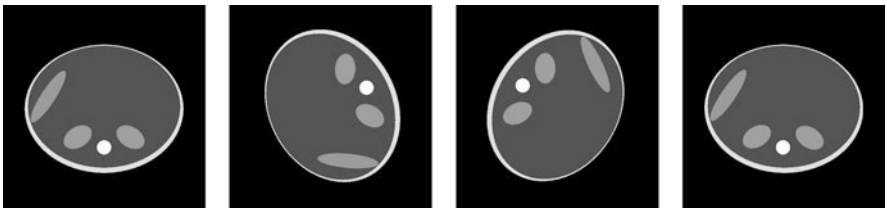

Fig. 4 Movement of phantom in $[0, \pi]$ for $t = 0, \frac{\pi}{2}, \frac{3\pi}{2}, \pi$. This movement is repeated in $[\pi, 2\pi]$

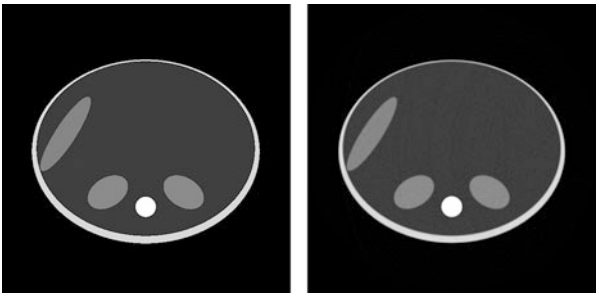

Fig. 5 Left: Ground-truth phantom. Right: Dynamic reconstruction under the 2π-periodic rotational motion model $\Gamma_t = B_t$

5.2 Non-periodic Motion

In our next examples, we consider the more realistic case of a non-periodic motion. In order to make clearly observable the visible (and invisible) singularities and the additional artifacts, which we expect from our theory (Sect. 4), we first consider a less complex phantom, namely a circle (see Fig. 6 (left)).

We start with an example that illustrates the following: Even in case of a full data, i.e. when all object singularities are encoded in the measured data, added artifacts can appear if the object is not in the same state at the beginning and the end of the scanning. As example, we consider the rotation matrix

$$G_t = \begin{pmatrix} \cos\left(-\frac{2}{3}t\right) & \sin\left(-\frac{2}{3}t\right) \\ -\sin\left(-\frac{2}{3}t\right) & \cos\left(-\frac{2}{3}t\right) \end{pmatrix}$$

and the associated motion model $\Gamma_t x = G_t x$, for $x \in \mathbb{R}^2$ and $t \in [0, 2\pi]$. In this example, the investigated object rotates in the opposite direction than the transducer. Thus, the transducer in relation to the object can perform at least one complete turn (even more) around the object, i.e. all object singularities are encoded in the dynamic data.

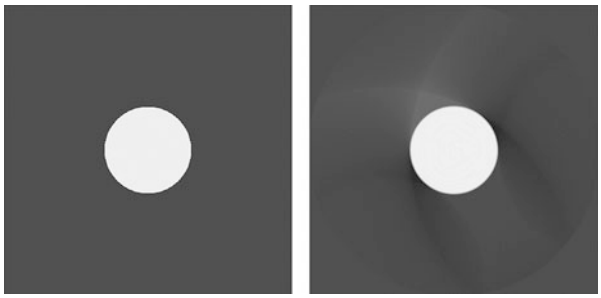

Fig. 6 Ground-truth phantom (left) and dynamic reconstruction (right)

Since $\Gamma_0 x = x$, the transducer position at $t = 0$ is $\theta(0) = (1, 0)^T$. Further, we have

$$\Psi_\Gamma(t, x) = \|\theta(t) - G_t^{-1} x\| = \|G_t \theta(t) - x\|,$$

since G_t is an isometry. Hence, the transducer position at $t = 2\pi$ with respect to the initial state of the object is given by $G_t\theta(t) = \theta\left(\frac{5t}{3}\right) = \theta\left(\frac{10}{3}\pi\right) = \theta\left(\frac{4}{3}\pi\right) = \left(-\frac{1}{2}, -\frac{\sqrt{3}}{2}\right)^T$. In the interval $[0, \frac{4}{3}\pi]$ the object is scanned twice and thus, all singularities of the object are visible in the reconstruction, see Fig. 6, where the contour of the circle is clearly visible.

However, we notice in the dynamic reconstruction Fig. 6 (right) the appearance of additional artifacts which occur because the motion is not 2π-periodic. We have

$$\mathrm{D}_x \Psi_\Gamma(t, x) = \frac{x - \theta\left(\frac{5t}{3}\right)}{\|\theta\left(\frac{5t}{3}\right) - x\|},$$

so any singularity (x, ξ) of f with

$$\xi = \sigma \mathrm{D}_x \Psi_\Gamma(t, x) = \sigma \frac{x - \theta\left(\frac{5t}{3}\right)}{\|\theta\left(\frac{5t}{3}\right) - x\|} = \tilde{\sigma}\left(x - \theta\left(\frac{5t}{3}\right)\right),$$

for $\tilde{\sigma} \in \mathbb{R} \setminus \{\mathbf{0}\}$ and $t \in \{0, 2\pi\}$ can create artifacts along the curve

$$\begin{aligned}\mathcal{S}_\Gamma(t, \Psi_\Gamma(t, x)) &= \left\{\tilde{x} \in \mathbb{R}^2 \ : \ \Psi_\Gamma(t, \tilde{x}) = \Psi_\Gamma(t, x)\right\} \\ &= \left\{\tilde{x} \in \mathbb{R}^2 \ : \ \|\theta\left(\tfrac{5t}{3}\right) - \tilde{x}\| = \|\theta\left(\tfrac{5t}{3}\right) - x\|\right\}.\end{aligned}$$

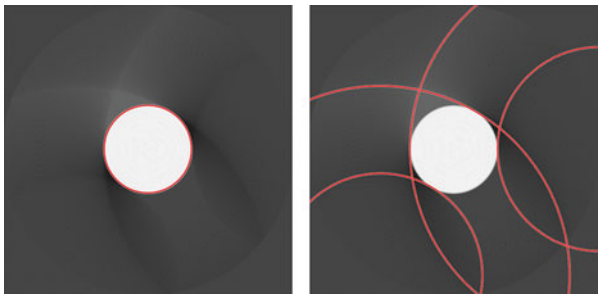

Fig. 7 Dynamic reconstruction with the visible singularities (left) and added artifacts (right) predicted by our theory highlighted in red

Hence, the artifacts appear along circle lines with centers $\theta(0) = (1,0)^T$ and $\theta\left(\frac{4}{3}\pi\right) = \left(-\frac{1}{2}, -\frac{\sqrt{3}}{2}\right)^T$, when a singularity of f is conormal to the circle. Figure 7 confirms that the additional artifacts predicted by our theory match the artifacts arising in our numerical reconstruction result.

Our next example shows that the dynamic behaviour of the investigated object can cause a limited-data problem. Here, we consider the rotation matrix

$$R_t = \begin{pmatrix} \cos\left(\frac{3}{4}t\right) & \sin\left(\frac{3}{4}t\right) \\ -\sin\left(\frac{3}{4}t\right) & \cos\left(\frac{3}{4}t\right) \end{pmatrix}$$

and the respective motion model $\Gamma_t x = R_t x$, for $x \in \mathbb{R}^2$ and $t \in [0, 2\pi]$. In this example, the object performs a rotational movement in the same direction as the rotation of the transducer.

The transducer position at $t = 0$ is $\theta(0) = (1,0)^T$ as in the example before and the source position at $t = 2\pi$ is now given by $R_t\theta(t) = \theta\left(\frac{t}{4}\right) = \theta\left(\frac{\pi}{2}\right) = (0,1)^T$. This scenario corresponds to the static limited angle case, where the object is only scanned for transducer locations associated to the interval $[0, \frac{3}{2}\pi] \subsetneq [0, 2\pi]$.

To validate our theory, we again compare the observed artifacts with their analytic characterization from Sect. 4.2. We have

$$\mathrm{D}_x \Psi_\Gamma(t,x) = \frac{x - \theta\left(\frac{t}{4}\right)}{\|\theta\left(\frac{t}{4}\right) - x\|},$$

so any singularity (x,ξ) of f with

$$\xi = \sigma \mathrm{D}_x \Psi_\Gamma(t,x) = \sigma \frac{x - \theta\left(\frac{t}{4}\right)}{\|\theta\left(\frac{t}{4}\right) - x\|} = \tilde{\sigma}\left(x - \theta\left(\tfrac{t}{4}\right)\right),$$

for $\tilde{\sigma} \in \mathbb{R} \setminus \{\mathbf{0}\}$ and $t \in \{0, 2\pi\}$ can create artifacts along the curve

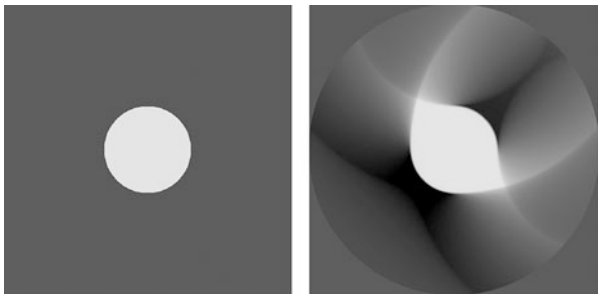

Fig. 8 Ground-truth phantom (left) and dynamic reconstruction (right)

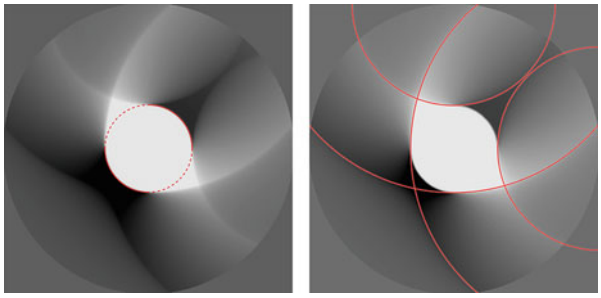

Fig. 9 Left: Visible (red solid line) and invisible (red dashed line) singularities. Right: Added artifacts (red)

$$\begin{aligned}\mathcal{S}_\Gamma(t, \Psi_\Gamma(t,x)) &= \left\{\tilde{x} \in \mathbb{R}^2 \ : \ \Psi_\Gamma(t,\tilde{x}) = \Psi_\Gamma(t,x)\right\} \\ &= \left\{\tilde{x} \in \mathbb{R}^2 \ : \ \|\theta\left(\tfrac{t}{4}\right) - \tilde{x}\| = \|\theta\left(\tfrac{t}{4}\right) - x\|\right\}.\end{aligned}$$

I.e. here, the artifacts appear along circle lines with centers $\theta(0) = (1,0)^T$ and $\theta\left(\frac{\pi}{2}\right) = (0,1)^T$, when a singularity of f is conormal to the circle, see Fig. 9 (right).

Since the visible singularities are given by

$$\begin{aligned}\mathcal{V}_{[0,2\pi]} &= \left\{\left(x, \tilde{\sigma}\left(x - \theta\left(\tfrac{t}{4}\right)\right)\mathrm{d}x\right) \ : \ t \in [0,2\pi],\ x \in \mathbb{R}^2,\ \tilde{\sigma} \in \mathbb{R} \setminus \{\mathbf{0}\}\right\} \\ &= \left\{\left(x, \tilde{\sigma}\left(x - \theta(t_v)\right)\mathrm{d}x\right) \ : \ t_v \in [0, \tfrac{\pi}{2}] \cup [\tfrac{3\pi}{2}, 2\pi],\ x \in \mathbb{R}^2,\ \tilde{\sigma} \in \mathbb{R} \setminus \{\mathbf{0}\}\right\},\end{aligned}$$

singularities (x, ξ) of f with direction $\xi = \sigma(x - \theta(t_\xi))$, $t_\xi \in (\frac{\pi}{2}, \frac{3\pi}{2})$, cannot be reconstructed from the dynamic data, see Figs. 8 and 9 (left).

As we can see in Fig. 9 visible singularities and added artifacts appear as predicted from our theory.

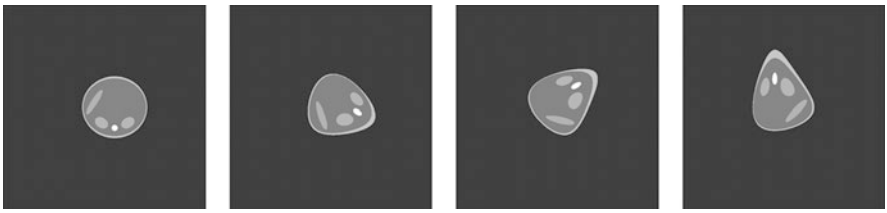

Fig. 10 Movement of phantom in $[0, 2\pi]$ for $t = 0,\ \frac{2\pi}{3},\ \frac{4\pi}{3},\ 2\pi$

This example shows, that the dynamic behavior can result in limited data problems (even though in the static case, the measured data would have been sufficient to recover all singularities).

After this detailed study, we finally want to provide one last example with the phantom from Sect. 5.1 and a more complex motion model, namely the non-affine (and non-periodic) deformation illustrated in Fig. 10.

Regarding the dynamic behavior, we consider

$$\Gamma_t x = Z_t A_t x,$$

with the rotation matrix

$$A_t = \begin{pmatrix} \cos\left(\frac{1}{2}t\right) & \sin\left(\frac{1}{2}t\right) \\ -\sin\left(\frac{1}{2}t\right) & \cos\left(\frac{1}{2}t\right) \end{pmatrix}$$

and the non-affine motion described by $Z_0 x = x$ and

$$(Z_t x)_i = \frac{(\sqrt[4]{5m_i(t)}x_i + 1)^5 - 1}{5\sqrt[4]{5m_i(t)}},$$

for $t \in (0, 2\pi]$ and $i = 1, 2$ with

$$m_1(t) = \sin\left(0.005\left(t\frac{N+1}{2\pi} - 1\right)\frac{3}{N}\right),$$
$$m_2(t) = \sin\left(0.007\left(t\frac{N+1}{2\pi} - 1\right)\frac{3}{N}\right).$$

Applying our reconstruction method to the corresponding dynamic data set provides an image showing the visible singularities of the initial object state as well as additional artifacts, see Fig. 11 (right), which are caused by the object singularities encoded at beginning and end of the scanning and which spread along the respective integration curves. In particular, we observe that the artifacts spread along deformed circle lines due to the non-affine motion model.

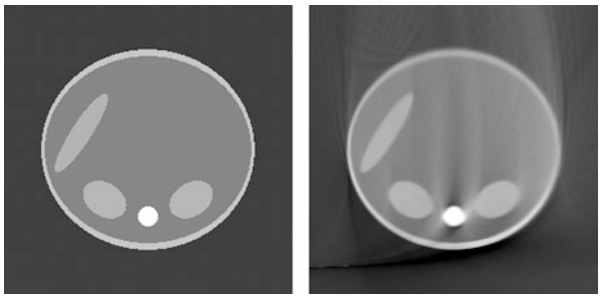

Fig. 11 Ground-truth phantom (left) and dynamic reconstruction (right)

6 Conclusion

In this chapter, we analysed the overall information content of dynamic tomography data using the framework of Fourier integral operators and microlocal analysis. In particular, we extended our previous results in [18] and [17] to a larger class of operators. Based on this analysis, we further provided a detailed characterization on what is visible in a respective reconstruction result assuming the motion is exactly known, which we illustrated with various numerical examples from dynamic photoacoustic tomography.

The developed theory can further be utilized to study the scenario where only incorrect motion information are available (accounting for instance for modelling or estimation errors). So far, this has been studied for instance in [15] for the specific example of dynamic computerized tomography. The gained insights could then serve as a guiding principle for the design of motion estimation protocols or additional artifact reduction strategies.

Acknowledgments The authors thank the referee for the thorough review and thoughtful comments. The work of the first and second authors was supported by the Deutsche Forschungsgemeinschaft under grant HA 8176/1-1. The first author thanks Tufts University for its hospitality and support during her visit which was essential to the work on this article. The work of the third author was partially supported by U.S. NSF grant DMS 1712207.

References

1. G. Ambartsoumian, R. Felea, V.P. Krishnan, C.J. Nolan, E.T. Quinto, Singular FIOs in SAR imaging, II: transmitter and receiver at different speeds. SIAM J. Math. Anal. **50**(1), 591–621 (2018)
2. G. Beylkin, The inversion problem and applications of the generalized Radon transform. Comm. Pure Appl. Math. **37**, 579–599 (1984)
3. L. Borg, J. Frikel, J.S. Jorgensen, E.T. Quinto, Analyzing reconstruction artifacts from arbitrary incomplete X-ray CT data. SIAM J. Imaging Sci. **11**, 2786–2814 (2018)

4. J. Chung, L. Nguyen, Motion estimation and correction in photoacoustic tomographic reconstruction. SIAM J. Imaging Sci. **10**(1), 216–242 (2017)
5. M. DeHoop, Microlocal analysis of seismic imaging, in *Inside - Out: Inverse Problems and Applications*, ed. by G. Uhlmann (MSRI Publications, Cambridge, 2003)
6. R. Felea, C. Nolan, Monostatic SAR with fold/cusp singularities. J. Fourier Anal. Appl. **21**(4), 799–821 (2015)
7. D. Finch, M. Haltmeier, Rakesh, Inversion of spherical means and the wave equation in even dimensions. SIAM J. Appl. Math. **68**(2), 392–412 (2007)
8. B. Frigyik, P. Stefanov, G. Uhlmann, The X-ray transform for a generic family of curves and weights. J. Geom. Anal. **18**, 81–97 (2008)
9. J. Frikel, E.T. Quinto, Characterization and reduction of artifacts in limited angle tomography. Inverse Probl. **29**(12), 125007 (2013)
10. J. Frikel, E.T. Quinto, Artifacts in incomplete data tomography with applications to photoacoustic tomography and sonar. SIAM J. Appl. Math. **75**, 703–725 (2015)
11. C. Grathwohl, P. Kunstmann, E.T. Quinto, A. Rieder, Microlocal analysis of imaging operators for effective common offset seismic reconstruction. Inverse Probl. **34**(11), 114001 (2018)
12. V. Guillemin, Some remarks on integral geometry. Technical Report, MIT (1975)
13. V. Guillemin, On some results of Gelfand in integral geometry. Proc. Symp. Pure Math. **43**, 149–155 (1985)
14. V. Guillemin, S. Sternberg, *Geometric Asymptotics* (American Mathematical Society, Providence, 1977)
15. B.N. Hahn, A motion artefact study and locally deforming objects in computerized tomography. Inverse Probl. **33**, 114001 (2017)
16. B.N. Hahn, Motion compensation strategies in tomography, in *Time-Dependent Problems in Imaging and Parameter Identification*, ed. by B. Kaltenbacher, T. Schuster, A. Wald (Springer, Cham, 2021), pp. 51–84
17. B.N. Hahn, M.L. Kienle-Garrido, An efficient reconstruction approach for a class of dynamic imaging operators. Inverse Probl. **35**, 094005 (2019)
18. B.N. Hahn, E.T. Quinto, Detectable singularities from dynamic Radon data. SIAM J. Imaging Sci. **9**, 1195–1225 (2016)
19. S. Holman, F. Monard, P. Stefanov, The attenuated geodesic X-ray transform. Inverse Probl. **34**(6), 064003 (2018)
20. L. Hörmander, Fourier integral operators, I. Acta Math. **127**, 79–183 (1971)
21. L. Hörmander, The analysis of linear partial differential operators. I: Distribution theory and Fourier analysis, in *Classics in Mathematics* (Springer, Berlin, 2003)
22. A. Katsevich, Motion compensated local tomography. Inverse Probl. **24**, 045012 (2008)
23. A. Katsevich, M. Silver, A. Zamyatin, Local tomography and the motion estimation problem. SIAM J. Imaging Sci. **4**, 200–219 (2011)
24. V.P. Krishnan, E.T. Quinto, Microlocal analysis in tomography, in *Handbook of Mathematical Methods in Imaging*, ed. by O. Scherzer, 2nd edn. (Springer, Berlin, 2015)
25. A.K. Louis, E.T. Quinto, Local tomographic methods in SONAR, in *Surveys on Solution Methods for Inverse Problems*, ed. by D. Colton, H. Engl, A. Louis, J. McLaughlin, W. Rundell (Springer, Vienna/New York, 2000), pp. 147–154
26. F. Natterer, *The Mathematics of Computerized Tomography* (B. G. Teubner, Stuttgart, 1986)
27. L.V. Nguyen, How strong are streak artifacts in limited angle computed tomography? Inverse Probl. **31**(5), 055003 (2015)
28. C.J. Nolan, M. Cheney, Synthetic Aperture inversion. Inverse Probl. **18**(1), 221–235 (2002)
29. T.J.P.M. Op 't Root, C.C. Stolk, M.V. de Hoop, Linearized inverse scattering based on seismic reverse time migration. J. Math. Pures Appl. **98**(2), 211–238 (2012)
30. E.T. Quinto, The dependence of the generalized Radon transform on defining measures. Trans. Amer. Math. Soc. **257**, 331–346 (1980)
31. E.T. Quinto, Singularities of the X-ray transform and limited data tomography in $\mathbb{R}^2$ and $\mathbb{R}^3$. SIAM J. Math. Anal. **24**, 1215–1225 (1993)

32. E.T. Quinto, O. Öktem, Local tomography in electron microscopy. SIAM J. Appl. Math. **68**, 1282–1303 (2008)
33. S. Rabieniaharatbar, Invertibility and stability for a generic class of Radon transforms with application to dynamic operators. J. Inverse Ill-Posed Probl. **27**, 469–486 (2018)
34. G. Rigaud, B.N. Hahn, 3D Compton scattering imaging and contour reconstruction for a class of Radon transforms. Inverse Probl. **34**(7), 075004 (2018)
35. W. Rudin, *Functional Analysis*. McGraw-Hill Series in Higher Mathematics (McGraw-Hill, New York, 1973)
36. P. Stefanov, G. Uhlmann, Is a curved flight path in SAR better than a straight one? SIAM J. Appl. Math. **73**(4), 1596–1612 (2013)
37. F. Trèves, *Introduction to Pseudodifferential and Fourier Integral Operators. Volume 1: Pseudodifferential Operators* (Plenum Press, New York, 1980)
38. F. Trèves, *Introduction to Pseudodifferential and Fourier Integral Operators. Volume 2: Fourier Integral Operators* (Plenum Press, New York, 1980)
39. J.W. Webber, S. Holman, Microlocal analysis of a spindle transform. Inverse Probl. Imaging **13**(2), 231–261 (2019)